bioRxiv preprint doi: https://doi.org/10.1101/223776; this version posted November 22, 2017. The copyright holder for this preprint (which was not certified by peer review) is the author/funder. All rights reserved. No reuse allowed without permission.

BCL11A interacts with SOX2 to control the expression of epigenetic regulators in lung squamous cell carcinoma

Kyren A. Lazarus[1,7], Fazal Hadi[1,7], Elisabetta Zambon[1,7], Karsten Bach[1,7], Maria-Francesca Santolla[1,3], Julie K. Watson[6], Lucia L. Correia[2], Madhumita Das[8], Rosemary Ugur[1,7], Sara Pensa[1,7], Lukas Becker[1], Lia S. Campos, Graham Ladds[1], Pentao Liu[4], Gerard Evan[2], Frank McCaughan[2], John Le Quesne[8,9,10], Joo-Hyeon Lee[6], Dinis Calado[5] and Walid T. Khaled[1,7]

1. Department of Pharmacology, University of Cambridge, Cambridge, UK

2. Department of Biochemistry, University of Cambridge, Cambridge, UK

3. Department of Pharmacy, Health and Nutritional Sciences, University of Calabria, Rende, Italy

4. Wellcome Trust Sanger Institute, Cambridge, UK

5. The Francis Crick Institute, London, UK

6. WT-MRC Stem Cell Institute, University of Cambridge, UK

7. Cambridge Cancer Centre, Cambridge, UK

8. MRC Toxicology Unit, Lancaster Road, Leicester

9. Cancer Research Centre, University of Leicester

10. University Hospitals Leicester NHS trust

Correspondence to: Walid T. Khaled (wtk22@cam.ac.uk)

bioRxiv preprint doi: https://doi.org/10.1101/223776; this version posted November 22, 2017. The copyright holder for this preprint (which was not certified by peer review) is the author/funder. All rights reserved. No reuse allowed without permission.

Abstract

Patients diagnosed with lung squamous cell carcinoma (LUSC) have limited targeted therapeutic options. We report here the identification and characterisation of the transcriptional regulator, *BCL11A,* as a LUSC oncogene. Analysis of cancer genomics datasets revealed *BCL11A* to be upregulated in LUSC but not lung adenocarcinoma (LUAD). We demonstrated that knockdown of *BCL11A* in LUSC cell lines abolished xenograft tumour growth and its overexpression *in vivo* led to lung airway hyperplasia and the development of reserve cell hyperplastic lesions. In addition, deletion of *Bcl11a* in the tracheal basal cells abolished the development of tracheosphere organoids while its overexpression led to solid tracheospheres with a squamous phenotype. At the molecular level we found *BCL11A* to be a target of SOX2 and we show that it is required for the oncogenic role of SOX2 in LUSC. Furthermore, we showed that *BCL11A* and SOX2 interact at the protein level and that together they co-regulated the expression of several transcription factors. We demonstrate that pharmacological inhibition of SETD8, a gene co-regulated by BCL11A and SOX2, alone or in combination with cisplatin treatment, shows significant selectivity to LUSC in comparison to LUAD cells. Collectively, these results indicate that the disruption of the BCL11A-SOX2 transcriptional program provides a future framework for the development of targeted therapeutic intervention for LUSC patients.

bioRxiv preprint doi: https://doi.org/10.1101/223776; this version posted November 22, 2017. The copyright holder for this preprint (which was not certified by peer review) is the author/funder. All rights reserved. No reuse allowed without permission.

Main

Lung cancer accounts for the highest rate of cancer related diagnosis and mortality worldwide[1]. Broadly, there are two major types of lung cancer; small cell lung cancer (SCLC) accounting for 15% of the cases and non-small cell lung cancer (NSCLC) accounting for 85% of cases[1]. NSCLC patients have a poor outcome in the clinic with only 15% of patients surviving five years or more[2]. At present NSCLC is defined histo-pathologically in the clinic into four broad categories: lung adenocarcinoma (LUAD), lung squamous cell carcinoma (LUSC), large cell carcinoma and undifferentiated non-small cell lung cancer. LUAD and LUSC are the most common types of NSCLC (90% of cases). LUSC accounts for more than 400,000 deaths worldwide each year[3] and unlike LUAD there are limited targeted therapies available for LUSC. Platinum-based chemotherapy remains the first-line treatment for LUSC and although the recent FDA approval of Necitumumab in combination with platinum-based chemotherapy for metastatic LUSC has shown positive signs, a great deal of work still needs to be done in this field[4].

At the cellular level, LUAD tends to originate from the secretory epithelial cells in the lung while LUSC usually originates from basal cells in the main and central airways[2]. At the molecular level LUAD is known to harbour mutations in epidermal growth factor receptor (EGFR), V-Ki-Ras2 Kirsten Rat Sarcoma Viral Oncogene Homolog (KRAS) and Anaplastic Lymphoma Receptor Tyrosine Kinase (ALK), which are also well modelled and studied both *in vitro* and *in vivo* (for review see [5,6]). On the other hand LUSC is less studied but it is known that amplifications of SRY (Sex Determining Region Y)-Box 2 (SOX2) tends to be present in 70-80% of patients[7-10].

bioRxiv preprint doi: https://doi.org/10.1101/223776; this version posted November 22, 2017. The copyright holder for this preprint (which was not certified by peer review) is the author/funder. All rights reserved. No reuse allowed without permission.

Recently, a detailed picture of the molecular differences between LUAD and LUSC has been made available through 'The Cancer Genome Atlas' (TCGA)[11,12]. To identify key drivers responsible for the differences between LUAD and LUSC we reanalysed the gene expression data from TCGA and focused on all 1500 transcriptional regulators in the genome. As reported previously *SOX2* was the most amplified gene in LUSC and its expression level was also significantly higher in LUSC vs. LUAD (Figure 1a and Supplementary Fig. 1a). The second most amplified locus in LUSC patients revealed by TCGA analysis contains the transcription factors *BCL11A* and *REL*[11,12]. *BCL11A* has been shown to be an oncogene in B-cell lymphoma and triple negative breast cancer[13-16].

We found that *BCL11A* expression levels were also significantly higher in LUSC vs. LUAD (Figure 1a and Supplementary Figure 1a). Moreover, the expression of both *BCL11A* and *SOX2* was significantly higher in LUSC but not LUAD tumour samples compared to patient matched normal samples (Figure 1b-c and Supplementary Figure 1b-c) supporting a driver role for these transcription factors in LUSC pathology. In contrast, *REL* expression was not different between LUSC and LUAD (Figure 1a-c and Supplementary Figure 1a-c) suggesting that *BCL11A* amplification is a key driving event in LUSC. This observation is supported by the recent report from the TRACERx (TRAcking Cancer Evolution through therapy (Rx)) study demonstrating the amplification of *BCL11A* as an early event in LUSC[17]. Furthermore, BCL11A IHC staining on LUAD (n=99) and LUSC (n=120) TMAs revealed little or no staining in 99% of LUAD patients. In contrast, 25% of LUSC patients had moderate staining and 24% of LUSC patients had strong staining, which is in agreement with previous IHC

bioRxiv preprint doi: https://doi.org/10.1101/223776; this version posted November 22, 2017. The copyright holder for this preprint (which was not certified by peer review) is the author/funder. All rights reserved. No reuse allowed without permission.

95 staining of NSCLC tumours[18]. This confirms our transcriptomic analyses indicating the
96 specificity of BCL11A in LUSC patients.
97 To determine if high levels of *BCL11A* expression are oncogenic in LUSC, we
98 performed shRNA mediated knockdown (KD) of *BCL11A* using two independent
99 shRNAs in two LUSC cell lines, LK2 and H520 (Supplementary Fig. 2a and b). We
100 first tested the clonogenic capacity of control or *BCL11A-KD* cells by seeding them into
101 matrigel for 3D colony formation assays. We found that *BCL11A-KD* cells had a
102 significant reduction in colony formation capacity (Supplementary Fig. 2c and d). We
103 then injected control or *BCL11A*-KD cells into immune compromised mice to test for
104 their tumour formation capacity and found a significant reduction in tumour burden
105 from *BCL11A-KD* cells compared to control cells (Fig 1e and f). In addition, we found
106 the squamous markers *KRT5* and *TP63* levels were significantly reduced in *BCL11A*-
107 KD cells (Supplementary Figure 2e-h) suggesting an integral role for *BCL11A* in
108 driving the LUSC phenotype. Moreover, to test if the role of BCL11A is context
109 dependant we knocked down *BCL11A* in an LUAD cell line H1792 and found no
110 change in 3D colony growth (Supplementary Figure 2i-j). Finally, at the molecular level
111 we found no change in the expression of *SOX2* in *BCL11A*-KD cells (Supplementary
112 Figure 2k, l).
113
114 To explore the role of BCL11A in lung biology, we utilised a novel Cre-inducible
115 mouse model that allows for the overexpression of *BCL11A*. Essentially, *BCL11A* was
116 inserted into the *Rosa26* locus with a LoxP-Stop-LoxP (*LSL*) cassette upstream, under
117 the control of a GAGG promoter, thus preventing the expression of *BCL11A* unless the
118 *LSL* is excised by Cre recombinase. To test the effect of *BCL11A* overexpression on
119 lung morphology, we allowed the *BCL11A*-overexpression ($BCL11A^{ovx}$) mice to inhale

bioRxiv preprint doi: https://doi.org/10.1101/223776; this version posted November 22, 2017. The copyright holder for this preprint (which was not certified by peer review) is the author/funder. All rights reserved. No reuse allowed without permission.

120 Adenovirus-Cre (Figure 2a). Eight months after infection, we analysed the lungs and
121 found an increase in airway hyperplasia (Figure 2b-c) accompanied by aggregates of
122 small hyperchromatic cells with irregular nuclei that represent reserve cell hyperplasia
123 (Figure 2b, arrows) which are precursors to squamous metaplasia[19]. IHC analysis of the
124 lungs from *BCL11A*^{ovx} also indicated an increase in positivity for the proliferative
125 marker Ki-67 (Supplementary Figure 3a) and Sox2 indicating a transition to squamous
126 differentiation (Supplementary Figure 3b). However, we found little difference in Cc10,
127 Krt5 and Trp63 staining at this stage (Supplementary Figure 3a and b).
128
129 To further investigate the role of *BCL11A* in LUSC, we employed a recently described
130 3D organoid culture system for basal cells (BCs) from the trachea, as they have been
131 suggested to be the cell of origin for LUSC[20]. BCs from human and mouse lungs have
132 higher expression of *BCL11A* when compared to the other epithelial compartments
133 (Supplementary Figure 4a and b) [21]. Therefore, we crossed the *BCL11A*^{ovx} mice to *R26-*
134 *CreERT2* mice, which allowed us to induce Cre recombination by the administration of
135 tamoxifen. In addition, we also used the previously reported *Bcl11a* conditional
136 knockout mouse under the control of *R26-CreERT2* (called *Bcl11a*^{CKO} from this point)
137 to elucidate the importance of BCL11A in organoid formation (Figure 2a).
138
139 We found that in contrast to the hollow organoids normally formed by wild-type BCs,
140 BCs from *BCL11A*^{ovx} mice formed solid organoid structures with no hollow lumen
141 suggesting hyper-proliferation and loss of organisation (Figure 2d). However, BCs from
142 *Bcl11a*^{cko} mice failed to form any organoid structures suggesting that *Bcl11a* is
143 necessary for stem cell potential in organoid formation (Figure 2d). Quantitative

bioRxiv preprint doi: https://doi.org/10.1101/223776; this version posted November 22, 2017. The copyright holder for this preprint (which was not certified by peer review) is the author/funder. All rights reserved. No reuse allowed without permission.

analysis revealed a significant decrease in organoid numbers from *Bcl11a*^{cko} BCs but no significant difference in *BCL11A*^{ovx} BCs (Supplementary Figure 4c-e).

H&E staining confirmed the hollowness of the organoids from the control mice which was in stark contrast to the filled organoids from the *BCL11A*^{ovx} mice (Figure 2e and Supplementary Figure 5). IF staining revealed that the *BCL11A*^{ovx} organoids were also positive for Ki-67 (Supplementary Figure 5), Sox2, Krt5, Trp63 and negative for the luminal marker Krt8 (Figure 2e and Supplementary Figure 6) indicating that BCL11A maintains a squamous phenotype.

Given the importance of SOX2 in driving LUSC[8,9] we next investigated if *BCL11A* is regulated by SOX2. To achieve this, we knocked down *SOX2* (*SOX2-KD*) in two LUSC cell lines using two independent shRNAs (Figure 3a, b and Supplementary Figure 7a, b). Similar to *BCL11A* we found that *SOX2-KD* cells had a significantly reduced colony and tumour formation abilities (Supplementary Figure 7c-f). At the molecular level we found a significant reduction in the expression levels of *BCL11A* and similar to *BCL11A-KD*, reduction in squamous markers *KRT5* and *TP63* in the *SOX2-KD* cells (Figure 3c, d and Supplementary Figure 7g-j).

To investigate if BCL11A is required for SOX2 mediated oncogenesis we introduced a doxycycline inducible *BCL11A* overexpression vector into *SOX2-KD* cell lines and found that *BCL11A* overexpression partially rescues the colony and tumour formation abilities of *SOX2-KD* cells (Figure 3e-h, f and Supplementary Figure 8a-c). These results suggest that BCL11A is partially responsible for some of SOX2's mediated transcriptional changes in LUSC cells.

bioRxiv preprint doi: https://doi.org/10.1101/223776; this version posted November 22, 2017. The copyright holder for this preprint (which was not certified by peer review) is the author/funder. All rights reserved. No reuse allowed without permission.

To understand how BCL11A and SOX2 contribute to the LUSC transcriptional programme we performed BCL11A and SOX2 ChIP-Seq analysis on LK2 cells in the presence or absence of BCL11A (*BCL11A-KD*) (Figure 3i). We identified 49,575 peaks for SOX2 and 4,904 peaks for BCL11A (Figure 3j and Supplementary Tables 1 and 2). Out of the 4,904 BCL11A peaks identified, 3,941 were not present in *BCL11A-KD* cells validating the true nature of BCL11A binding at these regions of the genome.

We then compared the BCL11A peaks and the SOX2 peaks and identified 958 peaks, which overlap suggesting co-regulation of these genes (Figure 3i and j). Subsequently, we identified the nearest genes to the common peaks (Supplementary Table 3) and performed Gene Ontology (GO) analysis to identify if these common peaks are enriched for specific biological process (Figure 3j). The top hits from the GO analysis revealed enrichment for transcriptional and epigenetic regulators including *SETD8, SKIL,* and *TBX2* (Figure 3k). We also found that SOX2 binds the *BCL11A* locus at multiple sites suggesting a strong direct regulation at the transcriptional level further supporting the data in Figure 3c and d (Figure 3k). BCL11A and SOX2 peaks on *SETD8*[22,23], *SKIL*[24], *TBX2*[25] and *BCL11A* were validated and confirmed by ChIP-qPCR (Supplementary Figure 9). The overlap of the ChIP-Seq peaks suggests a direct interaction between BCL11A and SOX2 proteins, which was confirmed in co-immunoprecipitation experiments on LK2 and H520 (Supplementary Figure 10a, b).

We then investigated the expression of *SETD8*, *SKIL* and *TBX2* in *BCL11A-KD* or *SOX2-KD* cells. Interestingly, we found a modest reduction in the expression of these genes in *BCL11A-KD*, which was more pronounced in *SOX2-KD* cells (Figure 4a-d; and

bioRxiv preprint doi: https://doi.org/10.1101/223776; this version posted November 22, 2017. The copyright holder for this preprint (which was not certified by peer review) is the author/funder. All rights reserved. No reuse allowed without permission.

Supplementary Figure 10c-j). This indicates that SOX2 has a major role in the regulation of *BCL11A*, which together with SOX2 drives the expression of key epigenetic regulators such as *SETD8*, *SKIL* and *TBX2*. This results suggest that disrupting the BCL11A-SOX2 transcriptional program might selectively target LUSC cells. To test this hypothesis we focused on SETD8 for its biology and the availability of multiple inhibitors. SETD8 is a member of the SET domain containing family and is known to catalyse the monomethylation of histone H4 Lys20[22,23] which is involved in recruiting signalling proteins or chromatin modifications[26]. In addition, SETD8 has been shown to play a role in maintaining skin differentiation[27] and is dysregulated in multiple cancer types[28-30].

We first assessed the expression of *SETD8* in multiple NSCLC cell lines and found that *SETD8* expression was significantly higher in LUSC cell lines (n=5) compared to LUAD cell lines (n=6) (Figure 4e) which was in correlation with the expression levels of *BCL11A* and *SOX2* (Figure 4f and g). Analysis of TCGA datasets revealed that SETD8 expression correlates with BCL11A and SOX2 expression in LUSC patients (Supplementary figure 11a and b). Next, we tested if LUSC lines are more sensitive to SETD8 inhibition. There are few SETD8 inhibitors but we focussed on one with proven cellular activity[31,32], named NSC663284. NSC663284 has also been reported as an inhibitor of Cdc25[33-35]. We treated all the NSCLC cell lines (n=11) with a range of NSC663284 concentrations (full details of setup in materials and methods) for 72 hours and measured cell viability. Remarkably, we found that LUSC cells had significantly lower IC_{50} (average 0.30 μM) compared to LUAD cells (average 7.65 μM) (Figure 4h and i). To understand if SETD8 inhibition would add a clinical benefit to patients, we tested the effect of combining NSC663284 and cisplatin. First, we found that cisplatin

bioRxiv preprint doi: https://doi.org/10.1101/223776; this version posted November 22, 2017. The copyright holder for this preprint (which was not certified by peer review) is the author/funder. All rights reserved. No reuse allowed without permission.

219 treatment for 24hrs alone affected LUSC and LUAD in a similar way with both cell
220 types demonstrating a similar IC_{50} (LUAD = 64.12 μM and LUSC = 31.67 μM) (Figure
221 4j and k). However, if we pre-treat NSCLC cell lines with NSC663284 for 48hrs and
222 then combine cisplatin with NSC663284 for a further 24hrs we found that LUSC (IC_{50}
223 = 4.66 μM) cells are more sensitive to cisplatin than LUAD cells (IC_{50} = 32.21 μM)
224 (Figure 4l, m).
225
226 In summary, we have demonstrated in this study that BCL11A is a LUSC oncogene.
227 We have shown that *BCL11A* is a key target of SOX2 and together they co-regulate the
228 expression of epigenetic regulators in LUSC cells. Our data suggests that disrupting the
229 BCL11A-SOX2 transcriptional program might selectively target LUSC cells. This was
230 demonstrated by the sensitivity of LUSC cell lines to the inhibition of the
231 BCL11A/SOX2 co-regulated gene *SETD8*. Collectively, these results indicate the key
232 oncogenic role of *BCL11A* in LUSC and provide a future framework for the
233 development of targeted therapeutic intervention for LUSC patients.
234
235
236

bioRxiv preprint doi: https://doi.org/10.1101/223776; this version posted November 22, 2017. The copyright holder for this preprint (which was not certified by peer review) is the author/funder. All rights reserved. No reuse allowed without permission.

Figure Legends

Figure 1. *BCL11A* is a lung squamous cell carcinoma (LUSC) oncogene

(a) Volcano plots of The Cancer Genome Atlas (TCGA) RNAseq data[11,12] indicating that *BCL11A* and *SOX2* are higher expressed in LUSC compared to lung adenocarcinoma (LUAD). The plot shows that *REL* is not differentially expressed in LUSC vs LUAD patients. The x-axis represents log2 expression fold-change (FC) in LUSC patients vs LUAD patients and the y-axis represents –log10(pValue). The vertical dashed lines represent FC = 1.0 and the horizontal dashed line represents p value = 0.01. **(b)** Volcano plots indicating that *BCL11A* and *SOX2* are differentially expressed in LUSC patients vs matched normal samples. The plot indicates that *REL* is not differentially expressed in LUSC vs matched normal samples **(c)** Volcano plots indicating that neither BCL11A, SOX2 nor *REL* are differentially expressed in LUAD patients vs matched normal. **(d)** Images and scoring of BCL11A IHC staining on LUAD and LUSC tumours (see Methods for scoring). Graph depicting reduction in tumour size observed when shRNA1 or shRNA2 transfected LK2 **(e)** and H520 **(f)** cells are injected subcutaneously into mice compared to control. Five mice per cell line were monitored for 25 days after which tumours were removed and measured. On the right are images showing actual tumours measured. Data presented as mean ± s.d. One way ANOVA with post Dunnett test performed, * indicates $p<0.05$ and ** $p<0.005$ and *** indicates $p<0.001$.

bioRxiv preprint doi: https://doi.org/10.1101/223776; this version posted November 22, 2017. The copyright holder for this preprint (which was not certified by peer review) is the author/funder. All rights reserved. No reuse allowed without permission.

Figure 2. *BCL11A* overexpression leads to thickening of the airways and abnormal organoid formation

(a) Schematic representing strategy to explore the role of *BCL11A in vivo* and *ex vivo*. Left Panel: Adenovirus-Cre was nasally administered to $BCL11A^{ovx}$ mice and the lungs were analysed after eight months. Right panel: for the tracheosphere organoid model, basal cells from the trachea of either $BCL11A^{ovx}$ or $BCL11A^{cko}$ mice were FACS sorted, embedded in matrigel and analysed after 15 days. Three independent mice were used for each experiment. **(b)** Images of airways from control and $BCL11A^{ovx}$. Arrows indicate small hyperchromatic cells with irregular nuclei. **(c)** Quantificaiton of airway epithelial layer hyperplasia from two control and $BCL11A^{ovx}$ mice. **(d)** Bright field images of organoids from $Bcl11a^{cko}$ and $BCL11A^{ovx}$ mice treated with vehicle or tamoxifen. **(e)** Sectioned organoids from $BCL11A^{ovx}$ mice stained with haematoxylin and eosin, BCL11A, Sox2, Krt5, Trp63 and Krt8. Scale bar indicates 50μm.

Figure 3. BCL11A and SOX2 occupy independent and common loci in the genome of LUSC cells

(a and b) Western blot showing SOX2 and BCL11A expression in *SOX2-KD* in LK2 **(a)** and H520 **(b)** cells transfected with control (scramble), shRNA1 or shRNA2 vectors. **(c and d)** *BCL11A* expression in *SOX2*-KD *LK2* **(c)** and *H520* **(d)** cells. **(e)** Western blot showing BCL11A rescue in *SOX2*-KD cells. Doxycycline (Dox) inducible *BCL11A* overexpression vector was transfected into control and *SOX2* shRNA1 LK2 cells and Dox treatment was performed for 48 hours. **(f)** Graph depicting 3D matrigel assay in control, *SOX2-KD* and *BCL11A* rescue cells indicating a partial rescue in *SOX2-KD*, *BCL11A* overexpressing cells. **(g)** Graph indicating partial rescue of tumour size from *BCL11A* overexpressing *SOX2-KD* cells injected subcutaneously. **(h)** Images of actual

bioRxiv preprint doi: https://doi.org/10.1101/223776; this version posted November 22, 2017. The copyright holder for this preprint (which was not certified by peer review) is the author/funder. All rights reserved. No reuse allowed without permission.

tumours measured. Four mice per cell line were monitored for 15 days after which tumours were removed and measured. Data presented as mean ± s.d. (n=4). One way Anova test performed, * indicates $p<0.05$ and ** $p<0.005$ and *** indicates $p<0.001$. **(i)** LK2 cell line either transfected with control or shRNA1 vectors were used for BCL11A and SOX2 ChIP-Seq. Heatmaps showing BCL11A only, SOX2 only or common peaks in BCL11A or SOX2 IP in control and *BCL11A*-KD cells. **(j)** Venn diagram indicating the overlap of BCL11A and SOX2 target genes in LK2 cells. BCL11A target genes were derived by comparing BCL11A IP in control vs BCL11A-KD cells. Any peaks lost in BCL11A-KD cells were considered as a 'true peak' and included as a bona fide BCL11A target gene. SOX2 target genes were derived from SOX2 IP in LK2 control cells. Image below show top five biological GO terms from GO analysis performed using DAVID. **(k)** IGV genome browser views for *SETD8*, *SKIL*, *TBX2* and *BCL11A*.

Figure 4. SETD8 inhibition preferentially sensitises LUSC cell lines to chemotherapy

(a-d) Graph depicting *SETD8* gene expression in LK2, H520 *BCL11A-KD* and LK2, H520 *SOX2 KD* cells. Data presented as mean ± s.d. (n=3). One way ANOVA with post Dunnett test performed, * indicates $p<0.05$ and ** $p<0.005$ and *** indicates $p<0.001$. **(e)** *SETD8* gene expression in NSCLC cell lines. **(f)** *BCL11A* gene expression in NSCLC cell lines. **(g)** *SOX2* gene expression in NSCLC cell lines. **(h)** Dose-response curves were derived by treating NSCLC cell lines with SETD8 inhibitor NSC663284. 1000 cells were seeded and allowed to recover for 24 hours. The inhibitor was then added at increasing concentrations to LUSC (red) and LUAD (blue) cells and Cell Titre (see Methods) assay was performed after 72 hours. **(i)** IC_{50} values were derived from the dose-response assay indicating LUSC cells are significantly more responsive to SETD8

bioRxiv preprint doi: https://doi.org/10.1101/223776; this version posted November 22, 2017. The copyright holder for this preprint (which was not certified by peer review) is the author/funder. All rights reserved. No reuse allowed without permission.

inhibition than LUAD cells. **(j)** Dose-response curves were derived by treating NSCLC cell lines with cisplatin as above. **(k)** IC_{50} values were derived from the dose-response assay indicating cisplatin effects LUSC and LUAD cells equally. **(l)** Dose-response curves derived from treating NSCLC cell lines with cisplatin and NSC663284 IC50 concentration for each cell line as above. **(m)** IC_{50} values were derived from the dose-response assay indicating SETD8 inhibition preferentially enhances cisplatin efficacy in LUSC cells. Data presented as mean ± s.d. (LUSC n=5 and LUAD n=6). Student's t-test performed, * indicates $p<0.05$ and ** $p<0.005$ and *** indicates $p<0.001$.

Supplementary Figure 1. BCL11A, SOX2, and REL expression in Lung TCGA dataset

(a) Violin plot showing *BCL11A*, *SOX2* and *REL* expression in LUSC vs LUAD. FPKM, fragments per kilobase per million mapped reads. **(b)** Violin plot showing *BCL11A*, *SOX2* and *REL* expression in LUSC tumour vs normal matched patients. **(c)** Violin plot showing *BCL11A*, *SOX2* and *REL* expression in LUAD tumour vs normal matched patients.

Supplementary Figure 2. BCL11A KD reduces squamous markers in LUSC cells

(a and b) qPCR and western blot shows *BCL11A* reduction in LK2 (**a**) and H520 **(b)** cells transfected with shRNA1 and shRNA2 vectors. **(c and d)** Comparison of colony numbers in 3D matrigel assay from control, shRNA1 or shRNA2 in LK2 **(c)** and **(d)** H520 cells. Data presented as mean ± s.d. (n=3). **(e and f)** *KRT5* expression is reduced in LK2 **(e)** and H520 (f) *BCL11A-KD* cells. **(g and h)** *TP63* expression is reduced in LK2 **(g)** and H520 (h) *BCL11A*-KD cells. **(i)** qPCR and western blot shows BCL11A reduction in H1792 cells transfected with shRNA1 and shRNA2 vectors. **(j)**

bioRxiv preprint doi: https://doi.org/10.1101/223776; this version posted November 22, 2017. The copyright holder for this preprint (which was not certified by peer review) is the author/funder. All rights reserved. No reuse allowed without permission.

Comparison of colony numbers in 3D matrigel assay from control, shRNA1 or shRNA2 in H1792 cells. **(k and l)** *SOX2* expression is unchanged in LK2 **(k)** and H520 **(l)** *BCL11A-KD* cells. Data presented as mean ± s.d. One way ANOVA with post Dunnett test performed, * indicates $p<0.05$ and ** $p<0.005$ and *** indicates $p<0.001$.

Supplementary Figure 3. Airways from the *BCLL1A^{ovx}* mice demonstrate proliferative preneoplastic lesions

(a) Immunohistochemistry for BCL11A, Ki67 and Cc10 expression in control vs BCL11A^{ovx} airways. BCL11A panel, arrows indicating positive staining especially in preneoplastic lesions. Ki67 panel, arrows indicating positive staining. **(b)** Sox2, Trp63 and Krt5 expression in control vs *BCL11A^{ovx}* airways. Scale bar indicates 50 μm.

Supplementary Figure 4. Organoids from *BCL11A^{ovx}* basal cells exhibit increase in squamous markers

(a) RNA-Seq data analysed from Weeden et al [21] indicating that in human samples FACS fraction labelled as proximal BCs has approximately 400 fold increase in human *BCL11A* levels in comparison to other epithelial fractions. **(b)** RNA-Seq data from the same dataset indicating that mouse *Bcl11a* is approximately 500-1000 fold higher in basal fractions compared to other epithelial subtypes. **(c, d and e)** Quantification of organoids in vehicle vs tamoxifen treated **(c)** BCL11A^{ovx}, **(d)** *BCL11A^{cko}* and **(e)** WT organoids.

Supplementary Figure 5. Organoids from the BCL11A^{ovx} basal cells display an abnormal proliferative phenotype

bioRxiv preprint doi: https://doi.org/10.1101/223776; this version posted November 22, 2017. The copyright holder for this preprint (which was not certified by peer review) is the author/funder. All rights reserved. No reuse allowed without permission.

Vehicle and tamoxifen treated BCL11A^{ovx} organoids stained with H&E, GFP (which is also expressed if the LSL is efficiently excised), Bcl11a and Ki67. Nuclei stained by DAPI illustrated in blue. Arrows indicate positive staining. Scale bar indicates 50μm.

Supplementary Figure 6. BCL11A overexpression inhibits organoid luminal differentiation

Vehicle and tamoxifen treated BCL11A^{ovx} organoids stained with Sox2, Krt5, Trp63 and Krt8. Nuclei stained by DAPI illustrated in blue. Arrows indicate positive staining. Scale bar indicates 50 μm.

Supplementary Figure 7. SOX2 KD affects LUSC cell lines tumourigenicity

(a and b) Graph showing *SOX2* expression in *SOX2-KD* LK2 (a) and H520 (b) cells. **(c and d)** Graph showing decrease in colony numbers in *SOX2-KD* LK2 **(c)** and H520 **(d)** cells. **(e and f)** Graph depicting reduction in tumour size observed when *SOX2* shRNA1 or shRNA2 transfected LK2 **(e)** and H520 **(f)** cells are injected subcutaneously into mice compared with control. Five (LK2) and four (H520) mice per cell line were monitored for 15 days after which tumours were removed and measured. On the right are images showing actual tumours measured. Data presented as mean ± s.d. One way ANNOVA with post Dunnett test performed, * indicates $p<0.05$ and ** $p<0.005$ and *** indicates $p<0.001$. **(g and h)** *KRT5* expression is reduced in LK2 **(g)** and H520 **(h)** *BCL11A*-KD cells. **(i and j)** *P63* expression is reduced in LK2 **(i)** and H520 **(j)** *BCL11A*-KD cells.

Supplementary Figure 8. BCL11A is required for SOX2 mediated LUSC phenotype

bioRxiv preprint doi: https://doi.org/10.1101/223776; this version posted November 22, 2017. The copyright holder for this preprint (which was not certified by peer review) is the author/funder. All rights reserved. No reuse allowed without permission.

(a and b) Graph showing *BCL11A* **(a)** and *SOX2* **(b)** expression in BCL11A rescue in *SOX2*-KD cells. Dox inducible *BCL11A* overexpression vector was transfected into control and *SOX2* shRNA1 LK2 cells and Dox treatment was performed for 48 hours. **(c)** Images from 3D matrigel experiment showing reduction in colony numbers after *SOX2-KD* and partial rescue after BCL11A overexpression.

Supplementary Figure 9. BCL11A and SOX2 bind to common loci on the genome

(a-h) ChIP-qPCR showing enrichment for the indicated primers on *SETD8, SKIL, TBX2* and *BCL11A* regions after Chip pull down using anti-BCL11A or anti-SOX2 antibodies in LK2 and H520 cell lines. **(i-l)** Schematic of amplicon locations for ChIP-qPCR validations performed in this study. Arrows represent location of primers used. Error bars represent mean ± s.e.m.; n = 3 (technical replicates).

Supplementary Figure 10. BCL11A and SOX2 co-regulate transcriptional regulators

(a and b) Co-Immunoprecipitation of endogenous BCL11A and SOX2 proteins in LK2 **(a)** and H520 **(b)** cell lines. **(c, d, g, h)** *SKIL* gene expression in *BCL11A*-KD or *SOX*-KD LK2 and H520 cell lines. **(e, f, I, j)** *TBX2* gene expression in *BCL11A*-KD or *SOX2*-KD LK2 and H520 cell lines. Data presented as mean ± s.d. (n=3). One way ANOVA with post Dunnett test performed, * indicates $p<0.05$ and ** $p<0.005$ and *** indicates $p<0.001$.

Supplementary Figure 11. *SETD8* correlates with *BCL11A* and *SOX2* in LUSC patients

bioRxiv preprint doi: https://doi.org/10.1101/223776; this version posted November 22, 2017. The copyright holder for this preprint (which was not certified by peer review) is the author/funder. All rights reserved. No reuse allowed without permission.

406 **(a)** Scatter plot showing *SETD8* and *BCL11A* expression in TCGA patient tumour
407 samples. **(b)** Scatter plot showing *SETD8* and *SOX2* expression in TCGA patient
408 tumour samples.
409
410
411

bioRxiv preprint doi: https://doi.org/10.1101/223776; this version posted November 22, 2017. The copyright holder for this preprint (which was not certified by peer review) is the author/funder. All rights reserved. No reuse allowed without permission.

412 **Materials and Methods**

413 **Mouse models**

414 All mice used in this study were maintained at the Sanger Institute or the University of
415 Cambridge. Housing and breeding of mice and experimental procedures were
416 performed according to the UK 1986 Animals Scientific Procedure Act and local
417 institute ethics committee regulations. The *BCL11A*^{ovx} allele was generated following a
418 strategy previously described[36]. Briefly, the *ROSA26* allele was targeted with a
419 construct containing human *BCL11A* cDNA preceded by a loxP flanked STOP cassette
420 and marked *eGFP* under the control of an internal ribosomal entry site (IRES)
421 downstream of the inserted cDNA and transgene transcription is controlled by the *CAG*
422 promoter. The generation of the *Bcl11a*^{cko} mice was described previously[16]. All mice
423 were 8–12 weeks of age at the time of experiments, and at least 3 mice per cohort were
424 used in each experiment. The primers used for genotyping are listed in Supplementary
425 Table 4.

426

427 **Mouse Tracheal Isolation and tracheoshpere culture**

428 Tracheae were incubated in 50 U/ml dispase (Sigma) for 45 minutes at 37^{o}C. 10 ml PBS
429 was injected through each trachea using a 25G 5/8" needle to flush out sheets of
430 epithelial cells. Cells were incubated in 0.25% trypsin for 5 minutes at 37^{o}C. Cells were
431 stained in PBS + 10%FBS + 1:100 anti-EpCAM PE-Cy7 (Biolegend) + 1:5000 DAPI
432 on ice for 20 minutes. Live EpCAM^{+ve} cells were isolated using a MoFlo sorter. 2500
433 cells were plated in 100µl 1:1 mix of Mouse Tracheal Epithelial Cell (MTEC)/Plus
434 media which is DMEM-Ham's F-12 (1:1 vol/vol), 15 mM HEPES, 3.6 mM sodium
435 bicarbonate, 4 mMl-glutamine, 100 U/ml penicillin, 100 µg/ml streptomycin, and 0.25
436 µg/ml fungizone; supplemented with 10 µg/ml insulin, 5 µg/ml transferrin, 0.1 µg/ml

bioRxiv preprint doi: https://doi.org/10.1101/223776; this version posted November 22, 2017. The copyright holder for this preprint (which was not certified by peer review) is the author/funder. All rights reserved. No reuse allowed without permission.

cholera toxin, 25 ng/ml epidermal growth factor (Becton-Dickinson, Bedford, MA), 30 μg/ml bovine pituitary extract, 5% FBS, and freshly added 0.01 μM retinoic acid[37] and growth factor reduced-Matrigel (Corning) per 24-well insert, in duplicate with 500 nM 4-hydroxy tamoxifen (Sigma) or ethanol (vehicle) for each mouse, and cultured for 15 days.

Cell lines

LK2, NCI-H520, NCI-H157, LUDLU1, SW900, NCI-H1792, NCI-H522, NCI-HCC78, A549, NCI-H1563, NCI-H1975 were all maintained in RPMI 1640 (Gibco), 10% FCS and 1% Penicillin/streptomycin in a 37^{o}C incubator with 5% CO_2.

ShRNA mediated knockdown

BCL11A shRNA sequences were obtained from TRC consortium (TRCN0000033449 and TRCN0000033453) and cloned into a piggyBac transposon vector (PB-H1-shRNA-GFP) as describe previously[38]. Sox2 shRNA sequences (TRCN0000355694 and TRCN0000257314) were also cloned as above. H520, H1792 and LK2 cells were transfected with 4.0 μg of respective vector using Lipofectamine 3000 or Lipofectamine LTX (Invitrogen). Cells were treated with G418 (400 μg/mL) (Gibco) for 5 days after which GFP^{+ve} cell were sorted using a Sony SH800 cell sorter (Sony, Tokyo, Japan) and cultured.

Transfection and 3D colony assays

The control or the *BCL11A* overexpression piggybac vectors were delivered into NSCLC cells using Lipofectamine LTX (Invitrogen). Transfected cells were maintained for 48 hours and then cultured in puromycin (1μg/ml). To induce BCL11A expression

bioRxiv preprint doi: https://doi.org/10.1101/223776; this version posted November 22, 2017. The copyright holder for this preprint (which was not certified by peer review) is the author/funder. All rights reserved. No reuse allowed without permission.

462 in LK2 *SOX2-KD* cells, doxycycline (Clonetech) was used at a final concentration of (1
463 μg/ml). 3D colony assays were performed by suspending 500 cells in matrigel (BD
464 Biosciences) and seeding this cell-matrigel suspension onto a 6-well plate. The plate
465 was then incubated for 15 minutes in 37^{o}C/5% CO_2 to allow hardening of suspension.
466 Growth media was added to the well and changed every 2-3 days for 20 days. All
467 experiments were performed in triplicates.
468
469 **Preparation of RNA**
470 RNA was extracted using the RNeasy mini kit (Qiagen). Cell cultures in T25 flasks
471 were first washed with cold PBS, and 350 μl of RLT was added. Cells were scraped,
472 passed through a 20G syringe five times and RNA was extracted using the RNeasy mini
473 kit (Qiagen) according to manufacturer instructions. DNA was degraded by adding 20U
474 Rnase-free DnaseI (Roche) for 30 minutes at room temperature. DnaseI treatment was
475 performed on columns.
476
477 **Preparation of cDNA and qRT-PCR**
478 1 μg of total RNA was diluted to a final volume of 11 μl. 2 μl of random primers
479 (Promega) were added after which the mixture was incubated at 65^{o}C for 5 mins. A
480 master mix containing Transcriptor Reverse Transcriptase (Roche), Reverse
481 Transcriptase buffer, 2 mM dNTP mix and RNasin Ribonuclease Inhibitors (Promega).
482 This mixture was incubated at 25 ^{o}C for 10 minutes, then 42^{o}C for 40 minutes and
483 finally 70^{o}C for 10 minutes. The resulting cDNA was then diluted 1:2.5 in H_2O for
484 subsequent use. qPCR was performed using a Step-One Plus Real-Time PCR System
485 (Thermofisher Scientific). Either Taqman (ThermoFisher Scientific) probes with GoTaq
486 Real Time qPCR Master Mix (Promega) or primers (Sigma) with PowerUp SYBR

bioRxiv preprint doi: https://doi.org/10.1101/223776; this version posted November 22, 2017. The copyright holder for this preprint (which was not certified by peer review) is the author/funder. All rights reserved. No reuse allowed without permission.

Green Master Mix (ThermoFisher Scientific) were used. All probe and primer details can be found in Supplementary Table 5 and 6. The enrichment was normalised with control mRNA levels of GAPDH and relative mRNA levels were calculated using the ΔΔCt method comparing to control group.

Western Blot

Cells were lysed using RIPA (Cell signalling) and protease inhibitors (Roche) as per manufacturer instructions. Total protein was measured using the bicinchoninic acid (BCA) method (Pierce Biotechnology). In total, 50 mg cell lysate was separated using 7.5% SDS-PAGE gels and transferred to PVDF membranes by electro-blotting. Membranes were blocked in 5% (w/v) milk in Tris-buffered saline containing 0.05% Tween-20 (TBST). Blots were then incubated at 4^{o}C overnight with primary antibodies as indicated, washed in TBST and subsequently probed with secondary antibodies for 1h at room temperature. ECL solution was then added to the membrane and analysed. Antibodies used were, anti-BCL11A (ab191401, Abcam, 1:3000), anti-SOX2 (ab97959, Abcam, 1:2000) and anti-TUBULIN (ab7291, Abcam, 1:10000).

Co-Immunoprecipitation

Cells were lysed using RIPA (Cell signalling) and protease inhibitors (Roche) as per the manufacturer's instructions. Total protein was measured using the BCA method as above (Pierce Biotechnology). Briefly, 500µg cell lysates were pre-cleared for 3h at 4°C to remove nonspecific binding. Then, the pre-cleared lysates were incubated with anti-BCL11A (Bethyl, A300-382A) and SOX2 (R&D Systems, AF2018) or control IgG at 4°C overnight. Next day 50µl of Dynabeads Protein G (Thermo Fisher Scientific) were

bioRxiv preprint doi: https://doi.org/10.1101/223776; this version posted November 22, 2017. The copyright holder for this preprint (which was not certified by peer review) is the author/funder. All rights reserved. No reuse allowed without permission.

added to each sample. After 3h, the complex was washed three times with RIPA buffer, and then analysed by Western Blot performed as described above.

Histology, Immunohistochemistry and Immunofluorescence

Cultured organoid were fixed with 4% paraformaldehyde in PBS for 4h at room temperature. After rinsing with PBS, fixed colonies were immobilised with Histogel (Thermo Scientific) for paraffin embedding. 5μm sections of lung tissues or embedded colonies were stained with haematoxylin and eosin (H&E) and immunostained with antibodies for BCL11A (IHC - ab191402, Abcam,1:1000), SOX2 (IHC – ab97959, 1:1000; IF – 14-9811-82, eBioscience, 1:200), Ki67 (IHC - MA5-14520, Thermo Scientific, 1:1000; IF - ab16667, Abcam, 1:300), GFP (IF - ab13970 Abcam, 1:1000), Keratin 8 (IF - TROMA-I, DSHB, 1:100), Keratin 5 (IHC – ab52635, Abcam, 1:1000; IF - 905501, Biolegend, 1:1000), P63 (IHC – ab735, Abcam, 1:200; IF – ab735, Abcam, 1:200), CCP10 (IHC – sc25555, Santa Cruz Biotechnology, 1:500). IHC secondary staining involved an HRP-conjugated donkey anti-rabbit or donkey anti-mouse secondary (1:250, Thermo Scientific) and were detected using DAB reagent (Thermo Scientific). IF secondary staining involved goat anti-chicken 488, goat anti-rabbit 647, goat anti-rat 647, goat anti-rabbit 488 and goat anti-mouse 647 (1:2000, Invitrogen). Nuclear stain was detected using Haematoxylin (IHC) or ProLong Gold Antifade Mountant DAPI (Thermofisher, P36941) (IF). IHC images were acquired using a Zeiss Axioplan 2 microscope and IF images were acquired using a Leica TCS SP5 confocal microscope and analysed on Image J.

Xenograft tumour assays

One million H520 and LK2 cells were suspended in 25% matrigel (BD Biosciences) and HBSS. This mixture was subcutaneously injected in 6-12 week old NSG mice. To

bioRxiv preprint doi: https://doi.org/10.1101/223776; this version posted November 22, 2017. The copyright holder for this preprint (which was not certified by peer review) is the author/funder. All rights reserved. No reuse allowed without permission.

induce BCL11A overexpression in *SOX2-KD* xenografts, mice were fed doxycycline pellets (Envigo, TD.01306, 625mg/kg). Mice were culled as specified in figure legends and resulting tumours were analysed.

ChIP-Seq and ChIP-qPCR

ChIP-Seq experiments were performed as described[39]. Antibodies used were BCL11A (Bethyl, A300-382A) and SOX2 (R&D Systems, AF2018). Briefly 2 x 15cm plates per cell line were formaldehyde crosslinked, nuclear fraction was isolated and chromatin sonicated using Bioruptor Pico (Diagenode). IP was performed using 100µl of Dynabeads Protein G (Thermo Fisher Scientific) and 10µg of antibody. The samples were then reverse crosslinked and DNA was eluted using Qiagen MinElute column. Sample was then processed either for sequencing or qPCR. Primers used for qPCR are listed in Supplementary Table 7.

Drug assays

SETD8 inhibitor NSC663284 (Cayman Chemical Company, 13303) was suspended using DMSO in 10mM stock concentration. Cisplatin (LKT Laboratories, C3374) was suspended in 154mM NaCl at a 3mM stock concentration. Cells were cultured as above and seeded at 1000 cells per 96-well plate and left to recover for 24h. The edges of the 96-well plate were avoided to ensure accuracy in measurement. For NSC663284, an initial dilution of 1:100 from stock was performed in RPMI media for the first concentration of 10-4M. Half log dilutions were performed in RPMI media reaching 10-6M and after which full log dilutions were performed reaching 10-10M. For cisplatin, initial dilution in RPMI media were made to achieve 100µM and 75µM. The 100µM solution was used to make the following solutions 50µM, 25µM, 12.5µM, 6.75µM,

bioRxiv preprint doi: https://doi.org/10.1101/223776; this version posted November 22, 2017. The copyright holder for this preprint (which was not certified by peer review) is the author/funder. All rights reserved. No reuse allowed without permission.

3.75μM, 1.5μM and 0.5μM. Cells were treated with vehicle for 48h after which the above doses of cisplatin were added. For cisplatin + NSC663284 experiment the NSC663284 IC50 concentration for each cell line was calculated and added initially for 48hrs and then added again along with the cisplatin dilution series as above for 24hrs. Data analysis for drug inhibitor assays was performed in GraphPad Prism 7.02 (San Diego, CA). Data were fitted to obtain concentration-response curves using the three-parameter logistic equation (for pIC50 values). Emax was constrained to 100% while the basal (Emin) parameter was contrained to 20%. Statistical differences were analyzed using one-way ANOVA or Student's t test as appropriate with post hoc Dunnett's multiple comparisons, and $p < 0.05$ was considered significant.

BCL11A IHC on patient tumours

TMAs contained LUAD (n=99) and LUSC (n=120) cases of archival primary pulmonary tumours collected under East Midlands NRES REC approved project (ref. 14/EM/1159). 1mm (n=3) cores are present per case which were initially scored (average nuclear staining intensity) as 0=neg, 1=weak, 2=moderate, 3=strong. A median score was calculated for each case and re classified as 0=neg, 1=moderate, 2=strong. All tissues and data are anonymised to the research team. IHC was performed using BCL11A antibody (ab19487, 1:200) with CC1 antigen retrieval using a Ventana discovery xt. Digital images of stained TMAs were scanned with a Nanozoomer RX instrument and scored on-screen by MD.

TCGA gene expression analysis

The TCGA data was accessed from the recount2 database[40] containing gene level count data from RNA-seq and clinical data from primary tumor samples from patients

bioRxiv preprint doi: https://doi.org/10.1101/223776; this version posted November 22, 2017. The copyright holder for this preprint (which was not certified by peer review) is the author/funder. All rights reserved. No reuse allowed without permission.

586 diagnosed with LUAD and LUSC, respectively. EdgeR[41] was used to test for
587 differential expression of transcription factors (as defined by Tfcheckpoint.org). For
588 this, compositional differences between samples were normalized using the trimmed
589 median of M-values method and a gene-specific dispersion was estimated for each gene.
590 A negative binomial generalized log-linear model was fit to each gene with the
591 covariates "plate+disease_type" (for the LUAD versus LUSC comparison) or
592 "patient+disease_type" (for the tumor versus normal comparison). A log-likelihood
593 ratio test was conducted to test whether the coefficient of the disease_type variable is
594 non-zero, followed by Benjamini-Hochberg adjustment of P values to account for
595 multiple testing. Plate A277 and A278 from the LUAD dataset were removed prior to
596 analysis as they showed a clear separation along the first component in a principal
597 component analysis from all other LUAD samples.
598
599 **ChIP-Seq analysis**
600 ChIP-Seq libraries were sequenced on illumina Hiseq2000 platform at the Wellcome
601 Sanger Institute. Each library was divided into two and sequenced on different lanes.
602 Reads were subsequently run through a pipeline at the sequencing facility to remove
603 adapter sequences and align to the reference genome among others. Alignment was
604 done using mem algorithm in BWA (version 0.7.15) and human_g1k_v37 was used as
605 the reference genome. Aligned and processed reads were received as compressed
606 CRAM files. Samtools (version 1.3.1) was used to decompress the CRAM files and
607 filter uniquely mapped reads in proper pairs. Next, reads from the two runs were
608 combined into a single BAM file using 'merge' function in samtools. Bedtools intersect
609 was then used to remove reads falling into blacklisted genomic regions or unplaced
610 genomic contigs of the GRCh37 assembly before marking and removing duplicate reads

bioRxiv preprint doi: https://doi.org/10.1101/223776; this version posted November 22, 2017. The copyright holder for this preprint (which was not certified by peer review) is the author/funder. All rights reserved. No reuse allowed without permission.

using MarkDuplicates function in Picard tools. Next, DownsampleSam in picard tools was used to sample ~105 million reads from each BAM file. Significantly enriched genomic regions relative to input DNA were identified using MACS2 (version 2.1.1.20160309) with p-value cutoff of 1.00e-05. Heatmaps generation: Mapped read counts were calculated in a 10bp window and normalised as RPKM (Reads Per Kilobase per Million mapped reads) using bamCoverage module from deeptools (version 2.5.1)[42]. This coverage file was used to compute score matrix ±1kb around peak summits using computeMatrix reference-point module (from deeptools version 2.5.1)[42]. Heatmaps of binding profiles around peak summits were then generated using plotHeatmap module in deeptools (version 2.5.1)[42]. Number of overlapping peaks between BCL11A and SOX2 and nearest downstream genes to peaks were determined using ODS and NDG utilities respectively in PeakAnnotator (version 1.4). For annotating nearest downstream genes, Homo sapiens GRCh37 (release 64) from ensembl was used.

Author contribution

K.L. designed and performed the majority of the experiments and analysed most of the data. F.H. analysed the ChIP-seq data. E.Z. performed the ChIP-qPCR experiments. K.B. analysed the TCGA data. S.P. performed some cell line work. R.U assisted with the BCL11A rescue experiment. M.F.S performed Co-IP experiment. L.B. measured the airway thickness. L.S.C. characterised the lung pathology of adenovirus mice. G.L designed and analysed the drug assays. J.K and J.H.L performed the tracheoshpere organoid experiment. L.L.C and F.M performed the mouse tissue IHC. M.D and J.LQ performed and analysed the BCL11A IHC on patient tumours. P.L. assisted with the NGS sequencing and provided the *Bcl11a*^{cko} mice. Adenovirus Cre administration was

bioRxiv preprint doi: https://doi.org/10.1101/223776; this version posted November 22, 2017. The copyright holder for this preprint (which was not certified by peer review) is the author/funder. All rights reserved. No reuse allowed without permission.

636 performed under G.E. supervision. D.C. generated the *BCL11A*^{ovx} mice. W.T.K
637 conceptualised and supervised the study. K.L and W.T.K wrote the manuscript.

638 **Acknowledgements**

639 We would like to thank the staff at Sanger Institute, Research Service Facility (RSF) for
640 their assistance. We would like to thank Dr. Catherine Wilson and Dr. Deborah
641 Burkhart (Department of Biochemistry, Cambridge) for her help with the Adenovirus
642 experiment. We would like to thank Dr. Emma Rawlins for helpful discussions and
643 comments. M.F.S was funded by Associazione Italiana per la Ricerca sul Cancro
644 (AIRC, 16719/2015). W.T.K is funded by a CRUK career establishment award
645 (C47525/A17348), University of Cambridge and Magdalene College, Cambridge. We
646 would also like to thank the Isaac Newton Trust for funding. G.L. was supported by the
647 BBSRC (Grant BB/M00015X/2).

648

649

bioRxiv preprint doi: https://doi.org/10.1101/223776; this version posted November 22, 2017. The copyright holder for this preprint (which was not certified by peer review) is the author/funder. All rights reserved. No reuse allowed without permission.

References

1. Siegel, R.L., Miller, K.D. & Jemal, A. Cancer statistics, 2017. *CA: A Cancer Journal for Clinicians* **67**, 7-30 (2017).
2. Chen, Z., Fillmore, C.M., Hammerman, P.S., Kim, C.F. & Wong, K.K. Non-small-cell lung cancers: a heterogeneous set of diseases. *Nature reviews. Cancer* **14**, 535-546 (2014).
3. Jemal, A.*, et al.* Global cancer statistics. *CA Cancer Journal for Clinicians* **61**, 69-90 (2011).
4. Pillai, R.N. & Ramalingam, S.S. Necitumumab: a new therapeutic option for squamous cell lung cancer? *Translational Lung Cancer Research* **3**, 382-383 (2014).
5. Kwon, M.-c. & Berns, A. Mouse models for lung cancer. *Molecular Oncology* **7**, 165-177 (2013).
6. The Cancer Genome Atlas Research, N. Comprehensive molecular profiling of lung adenocarcinoma. *Nature* **511**, 543-550 (2014).
7. McCaughan, F.*, et al.* Progressive 3q Amplification Consistently Targets SOX2 in Preinvasive Squamous Lung Cancer. *American Journal of Respiratory and Critical Care Medicine* **182**, 83-91 (2010).
8. Bass, A.J.*, et al.* SOX2 is an amplified lineage-survival oncogene in lung and esophageal squamous cell carcinomas. *Nat Genet* **41**, 1238-1242 (2009).
9. Hussenet, T.*, et al.* SOX2 Is an Oncogene Activated by Recurrent 3q26.3 Amplifications in Human Lung Squamous Cell Carcinomas. *PLOS ONE* **5**, e8960 (2010).
10. Lu, Y.*, et al.* Evidence That SOX2 Overexpression Is Oncogenic in the Lung. *PLOS ONE* **5**, e11022 (2010).
11. Network, T.C.G.A.R. Comprehensive genomic characterization of squamous cell lung cancers. *Nature* **489**, 519-525 (2012).
12. Campbell, J.D.*, et al.* Distinct patterns of somatic genome alterations in lung adenocarcinomas and squamous cell carcinomas. *Nat Genet* **48**, 607-616 (2016).
13. Khaled, W.T.*, et al.* BCL11A is a triple-negative breast cancer gene with critical functions in stem and progenitor cells. *Nat Commun* **6**(2015).
14. Tao, H.*, et al.* BCL11A expression in acute myeloid leukemia. *Leukemia Research* **41**, 71-75 (2016).
15. Weniger, M.A.*, et al.* Gains of the proto-oncogene BCL11A and nuclear accumulation of BCL11AXL protein are frequent in primary mediastinal B-cell lymphoma. *Leukemia* **20**, 1880-1882 (2006).
16. Yu, Y.*, et al.* Bcl11a is essential for lymphoid development and negatively regulates p53. *The Journal of Experimental Medicine* **209**, 2467 (2012).
17. Jamal-Hanjani, M.*, et al.* Tracking the Evolution of Non–Small-Cell Lung Cancer. *New England Journal of Medicine* **376**, 2109-2121 (2017).
18. Zhang, N.*, et al.* The BCL11A-XL expression predicts relapse in squamous cell carcinoma and large cell carcinoma. *Journal of Thoracic Disease* **7**, 1630-1636 (2015).
19. Idowu, M.O. & Powers, C.N. Lung cancer cytology: potential pitfalls and mimics - a review. *International Journal of Clinical and Experimental Pathology* **3**, 367-385 (2010).
20. Rock, J.R.*, et al.* Basal cells as stem cells of the mouse trachea and human airway epithelium. *Proceedings of the National Academy of Sciences* **106**, 12771-12775 (2009).
21. Weeden, C.E.*, et al.* Lung Basal Stem Cells Rapidly Repair DNA Damage Using the Error-Prone Nonhomologous End-Joining Pathway. *PLOS Biology* **15**, e2000731 (2017).
22. Nishioka, K.*, et al.* PR-Set7 Is a Nucleosome-Specific Methyltransferase that Modifies Lysine 20 of Histone H4 and Is Associated with Silent Chromatin. *Molecular Cell* **9**, 1201-1213 (2002).
23. Wu, S. & Rice, J.C. A new regulator of the cell cycle. *Cell Cycle* **10**, 68-72 (2011).

bioRxiv preprint doi: https://doi.org/10.1101/223776; this version posted November 22, 2017. The copyright holder for this preprint (which was not certified by peer review) is the author/funder. All rights reserved. No reuse allowed without permission.

24. Tecalco-Cruz, A.C., *et al.* Transforming Growth Factor-β/SMAD Target Gene SKIL Is Negatively Regulated by the Transcriptional Cofactor Complex SNON-SMAD4. *Journal of Biological Chemistry* **287**, 26764-26776 (2012).
25. Prince, S., Carreira, S., Vance, K.W., Abrahams, A. & Goding, C.R. Tbx2 Directly Represses the Expression of the p21 (WAF1) Cyclin-Dependent Kinase Inhibitor. *Cancer Research* **64**, 1669 (2004).
26. Lu, X., *et al.* The effect of H3K79 dimethylation and H4K20 trimethylation on nucleosome and chromatin structure. *Nat Struct Mol Biol* **15**, 1122-1124 (2008).
27. Driskell, I., *et al.* The histone methyltransferase Setd8 acts in concert with c-Myc and is required to maintain skin. *The EMBO Journal* **31**, 616-629 (2012).
28. Takawa, M., *et al.* Histone Lysine Methyltransferase SETD8 Promotes Carcinogenesis by Deregulating PCNA Expression. *Cancer Research* **72**, 3217 (2012).
29. Shi, X., *et al.* Modulation of p53 Function by SET8-Mediated Methylation at Lysine 382. *Molecular Cell* **27**, 636-646 (2007).
30. Yang, F., *et al.* SET8 promotes epithelial–mesenchymal transition and confers TWIST dual transcriptional activities. *The EMBO Journal* **31**, 110 (2011).
31. Blum, G., *et al.* Small-Molecule Inhibitors of SETD8 with Cellular Activity. *ACS Chemical Biology* **9**, 2471-2478 (2014).
32. Milite, C., *et al.* The emerging role of lysine methyltransferase SETD8 in human diseases. *Clinical Epigenetics* **8**, 102 (2016).
33. Pu, L., Amoscato, A.A., Bier, M.E. & Lazo, J.S. Dual G1 and G2 Phase Inhibition by a Novel, Selective Cdc25 Inhibitor 7-Chloro-6-(2-morpholin-4-ylethylamino)- quinoline-5,8-dione. *Journal of Biological Chemistry* **277**, 46877-46885 (2002).
34. Brisson, M., *et al.* Redox Regulation of Cdc25B by Cell-Active Quinolinediones. *Molecular Pharmacology* **68**, 1810 (2005).
35. Lazo, J.S., *et al.* Discovery and Biological Evaluation of a New Family of Potent Inhibitors of the Dual Specificity Protein Phosphatase Cdc25. *Journal of Medicinal Chemistry* **44**, 4042-4049 (2001).
36. Sasaki, Y., *et al.* Canonical NF-κB Activity, Dispensable for B Cell Development, Replaces BAFF-Receptor Signals and Promotes B Cell Proliferation upon Activation. *Immunity* **24**, 729-739 (2006).
37. You, Y., Richer, E.J., Huang, T. & Brody, S.L. Growth and differentiation of mouse tracheal epithelial cells: selection of a proliferative population. *American Journal of Physiology - Lung Cellular and Molecular Physiology* **283**, L1315 (2002).
38. Khaled, W.T., *et al.* BCL11A is a triple-negative breast cancer gene with critical functions in stem and progenitor cells. **6**, 5987 (2015).
39. Schmidt, D., *et al.* ChIP-seq: Using high-throughput sequencing to discover protein–DNA interactions. *Methods* **48**, 240-248 (2009).
40. Collado-Torres, L., *et al.* Reproducible RNA-seq analysis using recount2. *Nat Biotech* **35**, 319-321 (2017).
41. Robinson, M.D., McCarthy, D.J. & Smyth, G.K. edgeR: a Bioconductor package for differential expression analysis of digital gene expression data. *Bioinformatics* **26**, 139-140 (2010).
42. Ramírez, F., Dündar, F., Diehl, S., Grüning, B.A. & Manke, T. deepTools: a flexible platform for exploring deep-sequencing data. *Nucleic Acids Research* **42**, W187-W191 (2014).

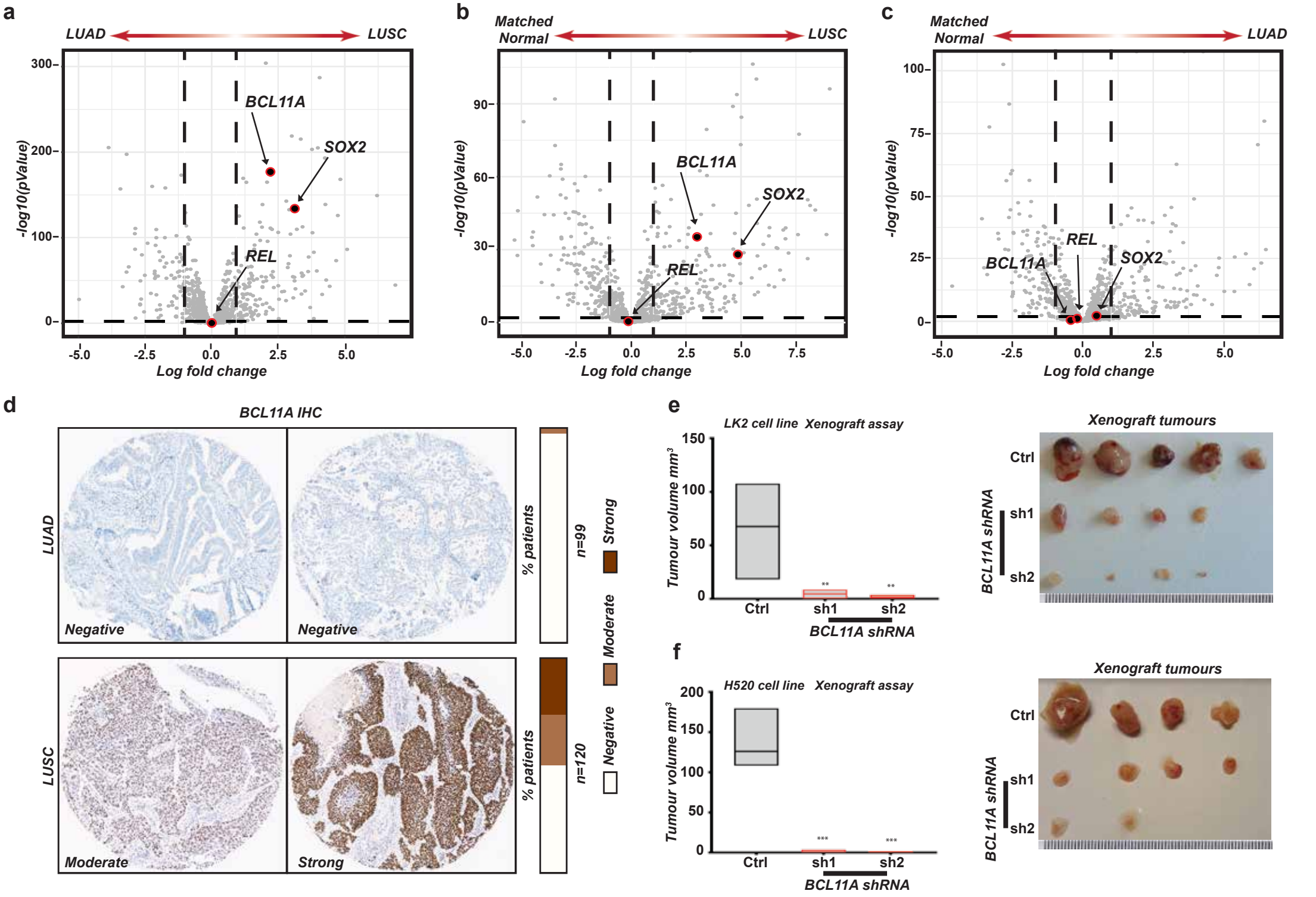
a
LUAD
LUSC
BCL11A
SOX2
REL
-log10(pValue)
Log fold change
b
Matched Normal
LUSC
BCL11A
SOX2
REL
-log10(pValue)
Log fold change
c
Matched Normal
LUAD
REL
BCL11A
SOX2
-log10(pValue)
Log fold change
d
BCL11A IHC
LUAD
Negative
Negative
LUSC
Moderate
Strong
% patients
n=99
n=120
Strong
Moderate
Negative
e
LK2 cell line Xenograft assay
Tumour volume mm3
Ctrl
sh1
sh2
BCL11A shRNA
Xenograft tumours
BCL11A shRNA
f
H520 cell line Xenograft assay
Tumour volume mm3
Ctrl
sh1
sh2
BCL11A shRNA
Xenograft tumours
BCL11A shRNA

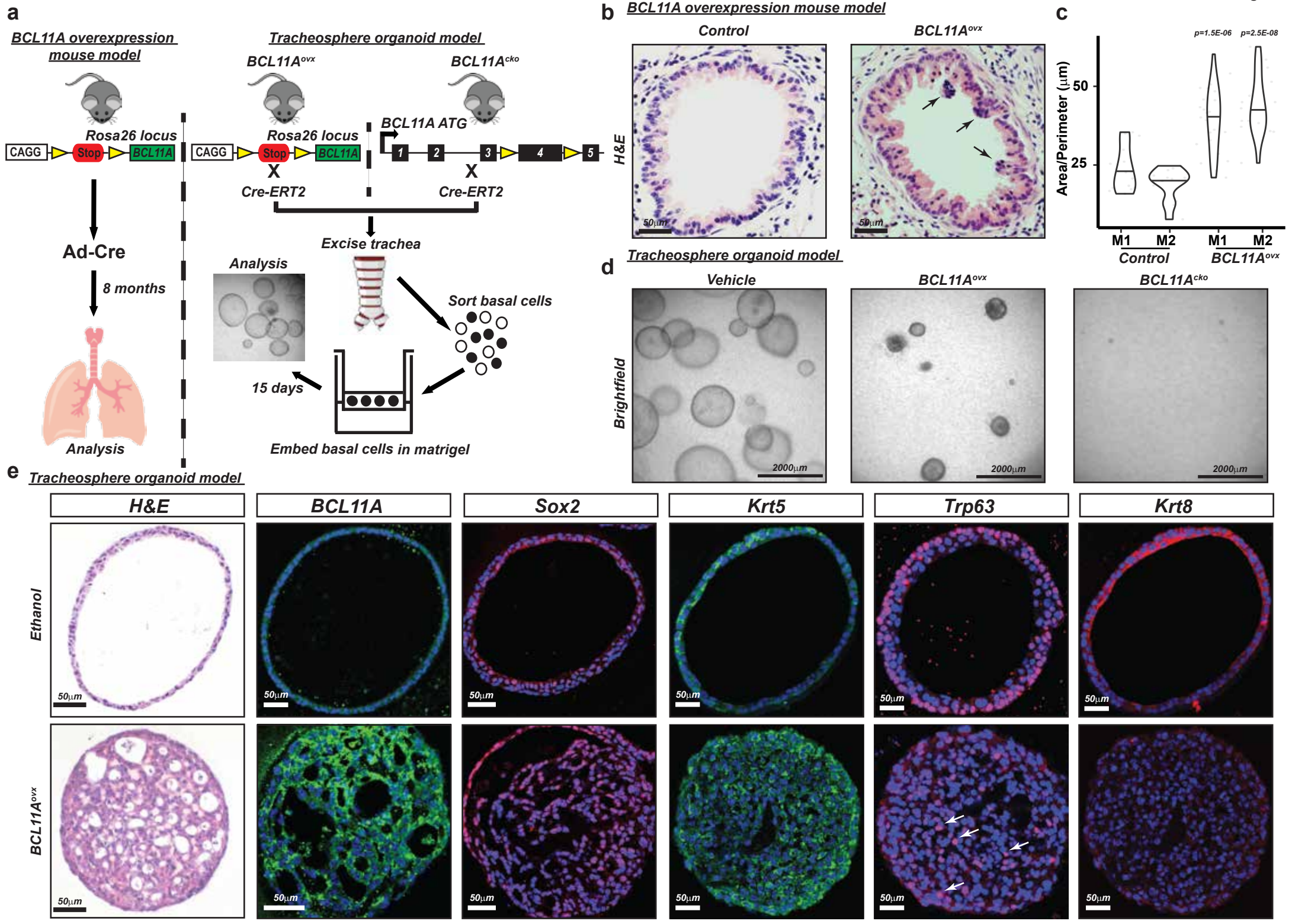
a
BCL11A overexpression mouse model
Tracheosphere organoid model
BCL11A^ovx
BCL11A^cko
Rosa26 locus
CAGG
Stop
BCL11A
BCL11A ATG
1
2
3
4
5
X
Cre-ERT2
Ad-Cre
8 months
Analysis
Excise trachea
Sort basal cells
15 days
Embed basal cells in matrigel
b
BCL11A overexpression mouse model
Control
BCL11A^ovx
H&E
50μm
c
p=1.5E-06
p=2.5E-08
Area/Perimeter (μm)
50
25
M1
M2
M1
M2
Control
BCL11A^ovx
d
Tracheosphere organoid model
Vehicle
BCL11A^ovx
BCL11A^cko
Brightfield
2000μm
e
Tracheosphere organoid model
H&E
BCL11A
Sox2
Krt5
Trp63
Krt8
Ethanol
BCL11A^ovx
50μm

bioRxiv preprint doi: https://doi.org/10.1101/223776; this version posted November 22, 2017. The copyright holder for this preprint (which was not certified by peer review) is the author/funder. All rights reserved. No reuse allowed without permission.

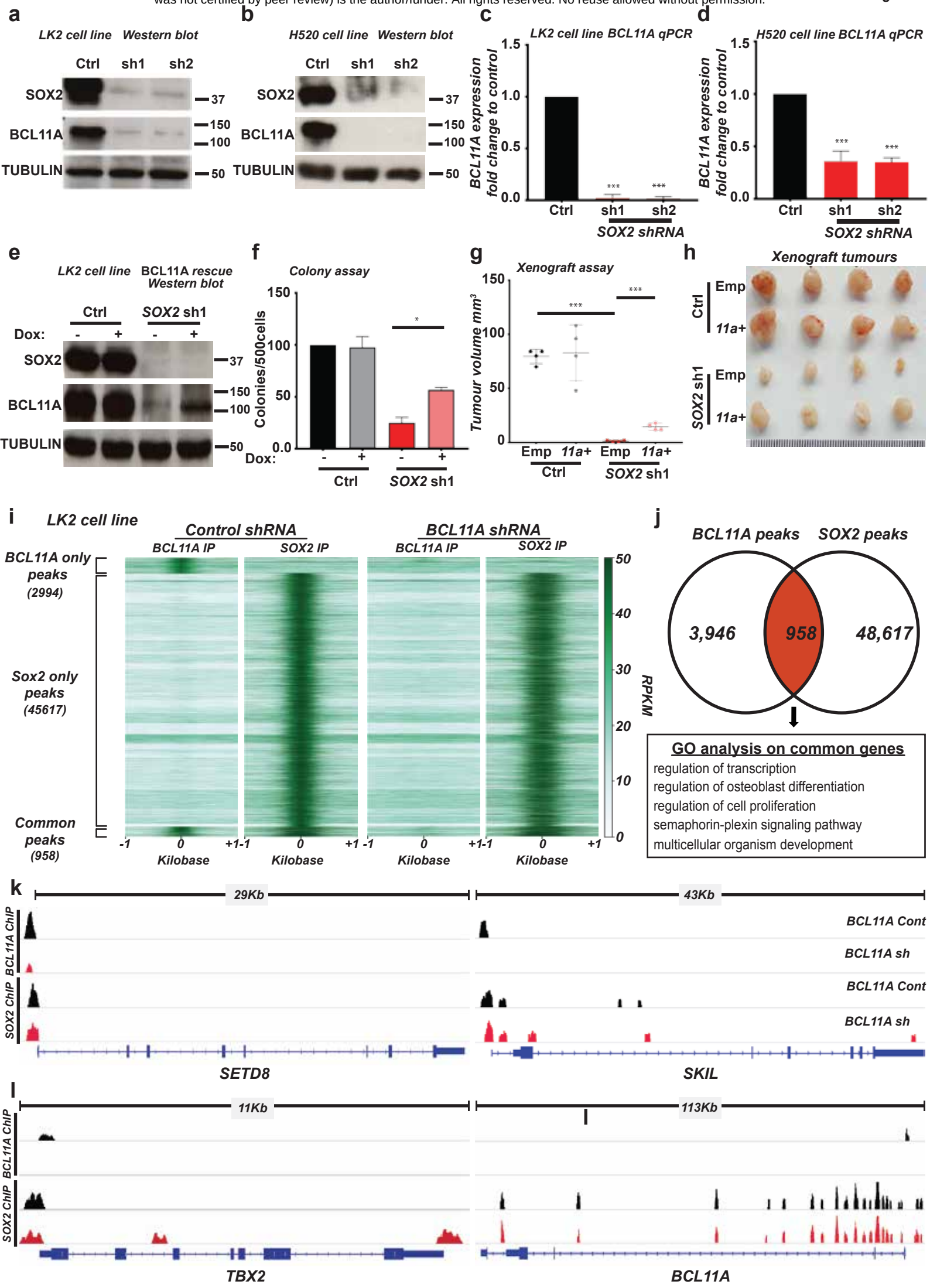

bioRxiv preprint doi: https://doi.org/10.1101/223776; this version posted November 22, 2017. The copyright holder for this preprint (which was not certified by peer review) is the author/funder. All rights reserved. No reuse allowed without permission.

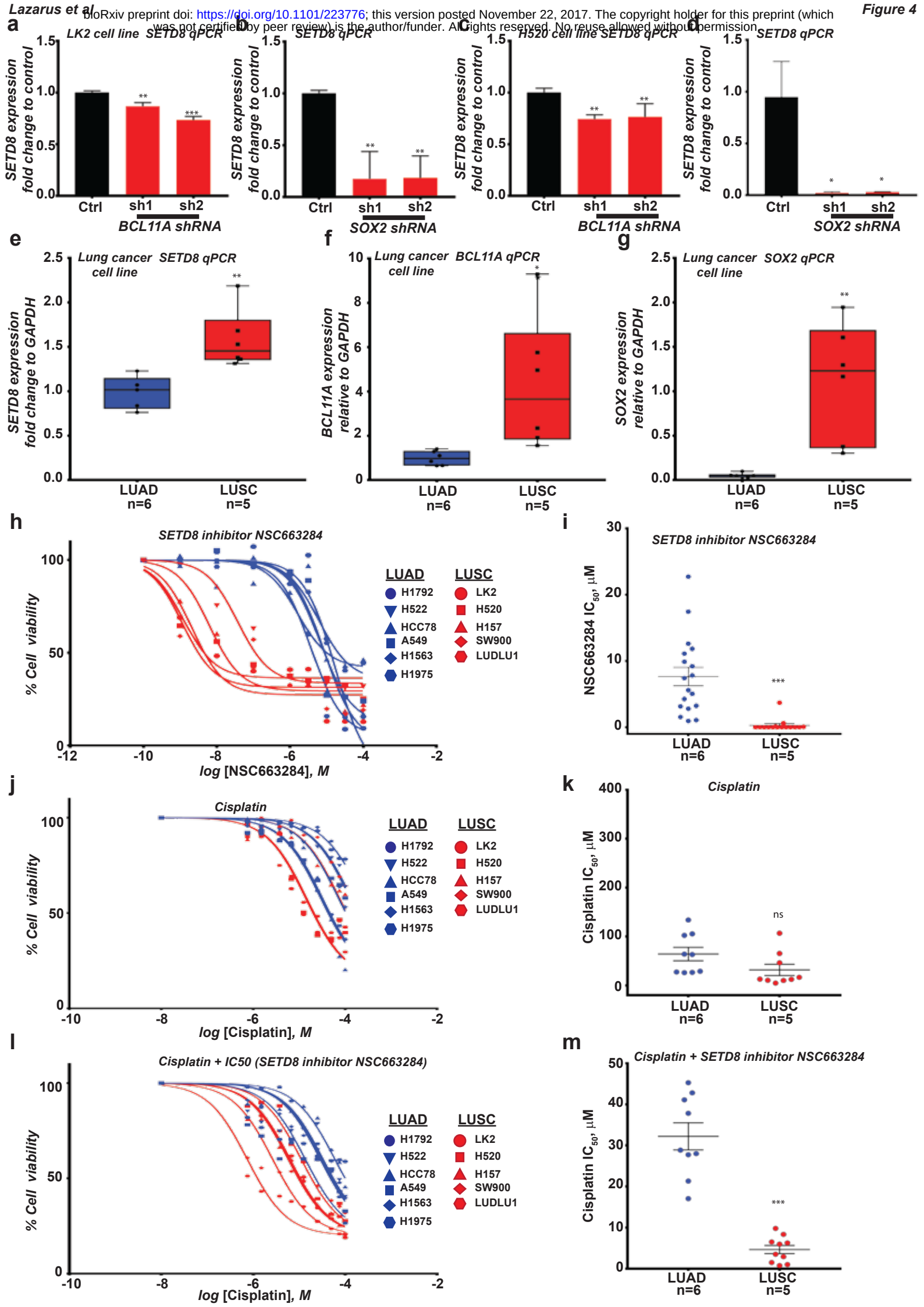

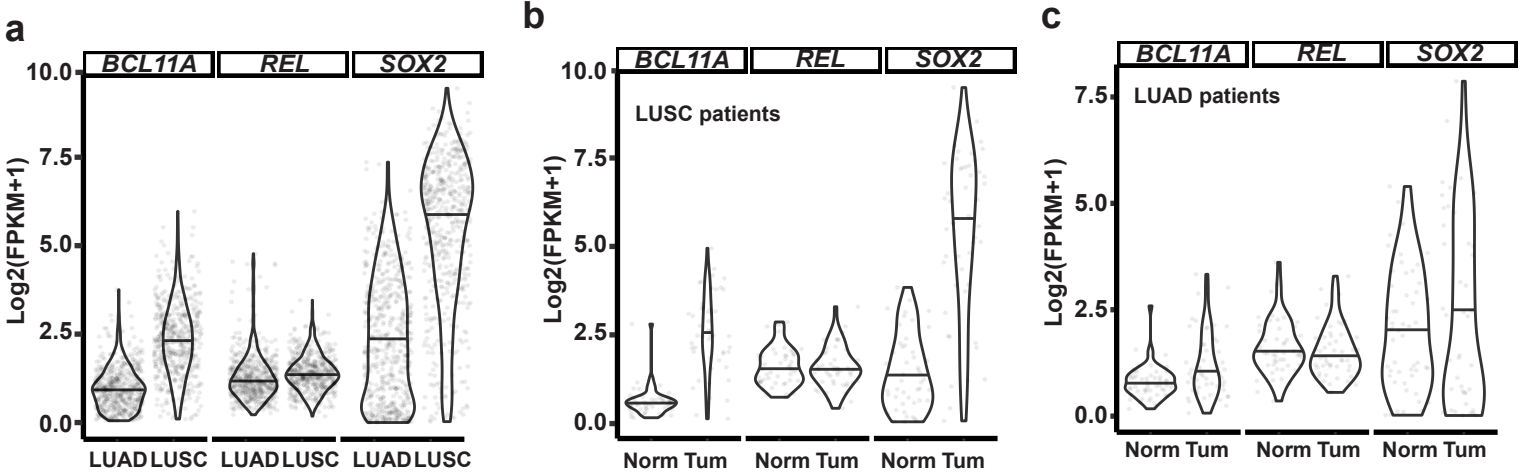
a
BCL11A
REL
SOX2
Log2(FPKM+1)
10.0
7.5
5.0
2.5
0.0
LUAD LUSC LUAD LUSC LUAD LUSC
b
BCL11A
REL
SOX2
LUSC patients
Log2(FPKM+1)
Norm Tum Norm Tum Norm Tum
c
BCL11A
REL
SOX2
LUAD patients
Log2(FPKM+1)
Norm Tum Norm Tum Norm Tum

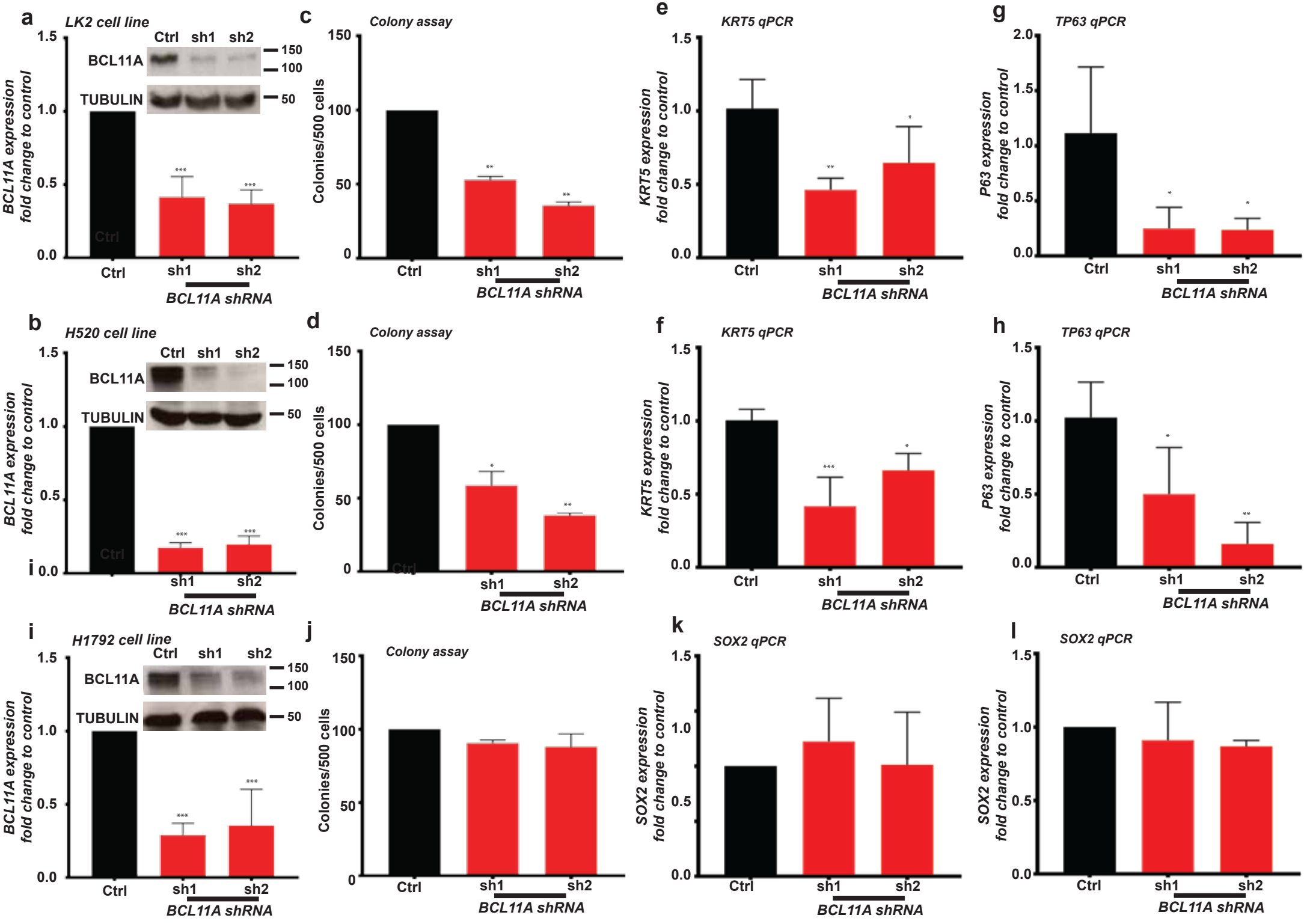
a
LK2 cell line
Ctrl sh1 sh2
BCL11A
TUBULIN
150
100
50
BCL11A expression fold change to control
Ctrl
sh1
sh2
BCL11A shRNA
b
H520 cell line
c
Colony assay
Colonies/500 cells
d
e
KRT5 qPCR
KRT5 expression fold change to control
f
g
TP63 qPCR
P63 expression fold change to control
h
i
H1792 cell line
j
k
SOX2 qPCR
SOX2 expression fold change to control
l

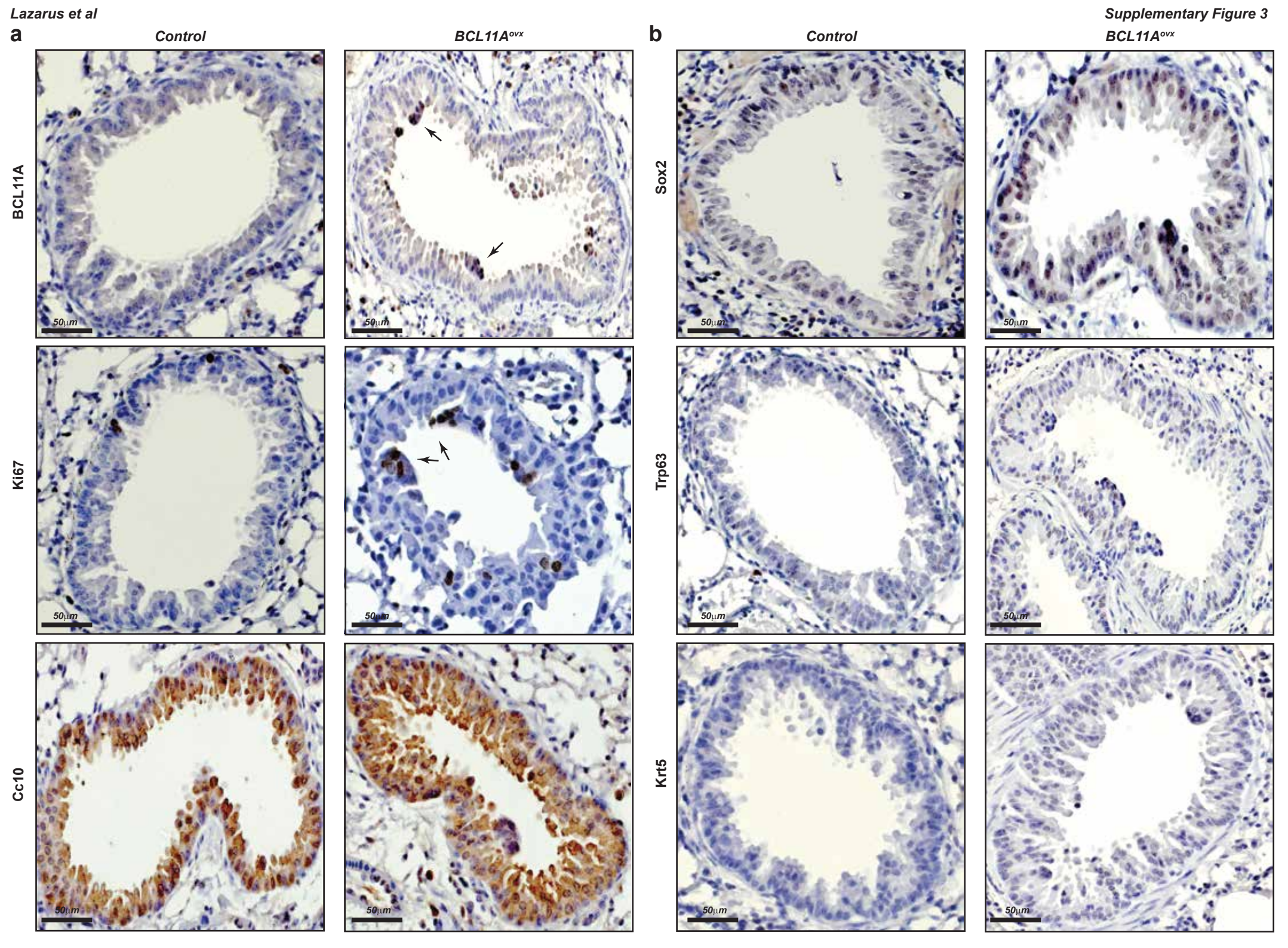
a
Control
BCL11A^ovx
BCL11A
Ki67
Cc10
b
Control
BCL11A^ovx
Sox2
Trp63
Krt5
50μm

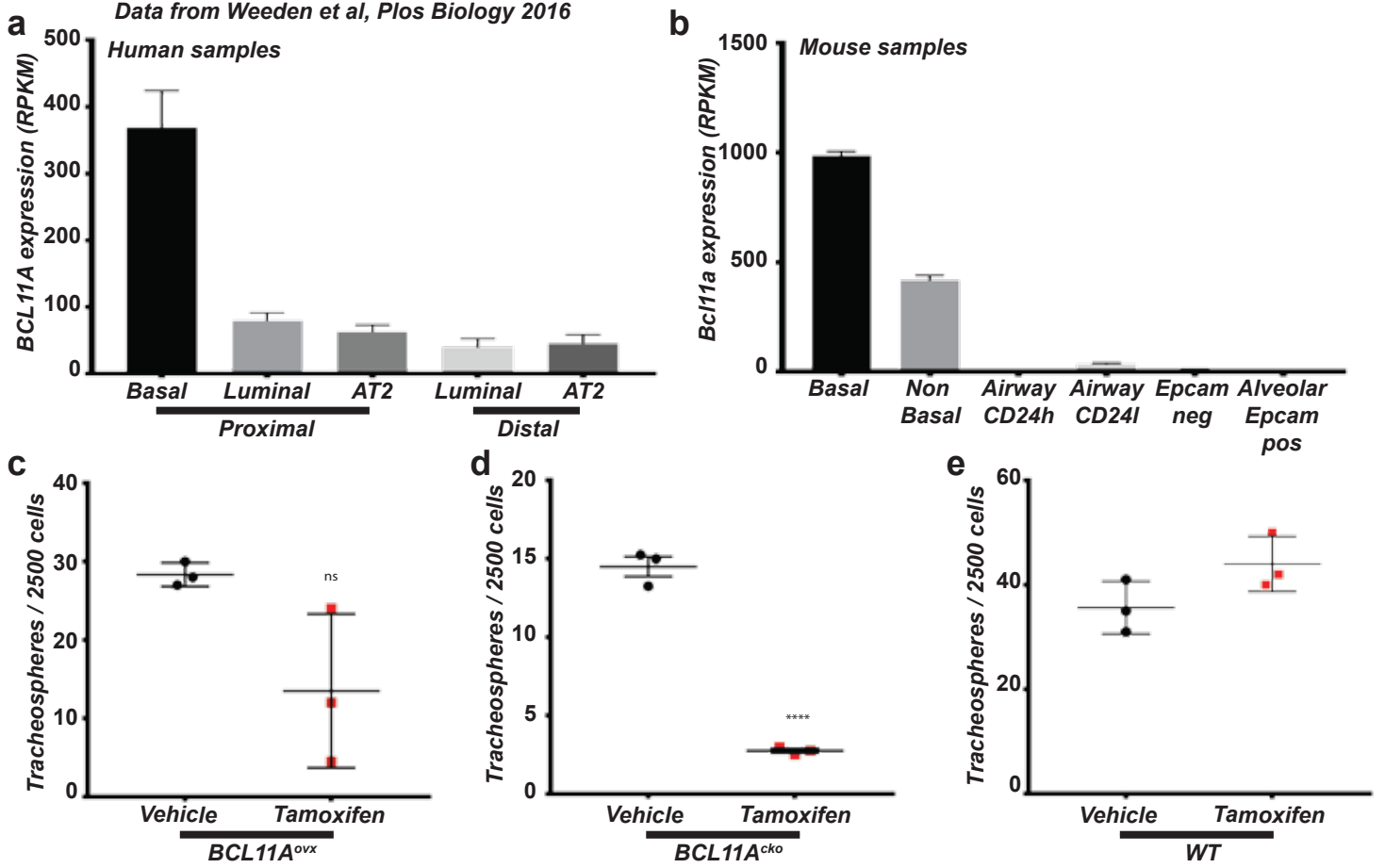
a
Data from Weeden et al, Plos Biology 2016
Human samples
BCL11A expression (RPKM)
500
400
300
200
100
0
Basal
Luminal
AT2
Luminal
AT2
Proximal
Distal
b
Mouse samples
Bcl11a expression (RPKM)
1500
1000
500
0
Basal
Non Basal
Airway CD24h
Airway CD24l
Epcam neg
Alveolar Epcam pos
c
Tracheospheres / 2500 cells
40
30
20
10
0
ns
Vehicle
Tamoxifen
BCL11Aovx
d
Tracheospheres / 2500 cells
20
15
10
5
0
****
Vehicle
Tamoxifen
BCL11Acko
e
Tracheospheres / 2500 cells
60
40
20
0
Vehicle
Tamoxifen
WT

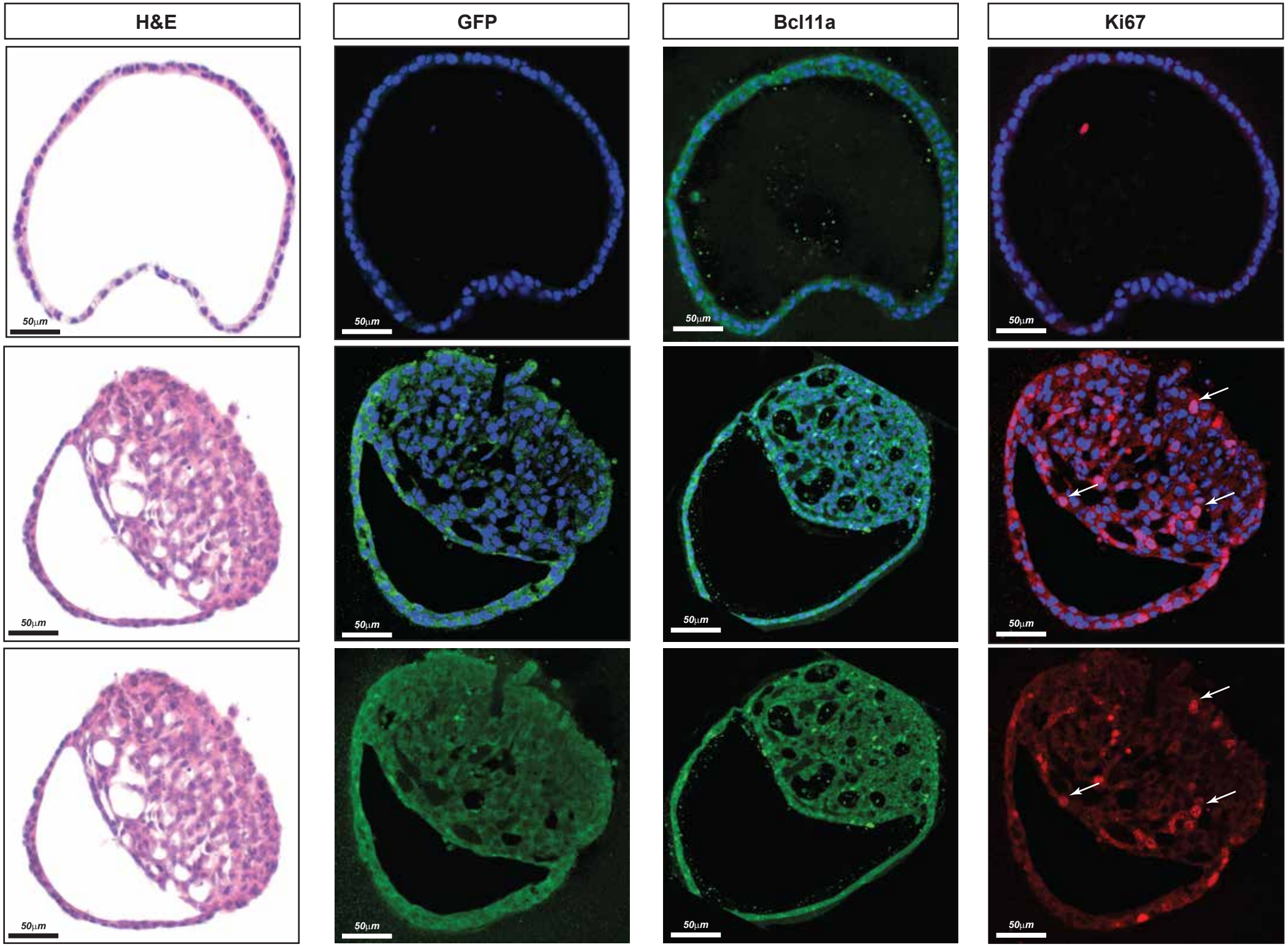
H&E
GFP
Bcl11a
Ki67
Vehicle
BCL11A^ovx
BCL11A^ovx
50μm

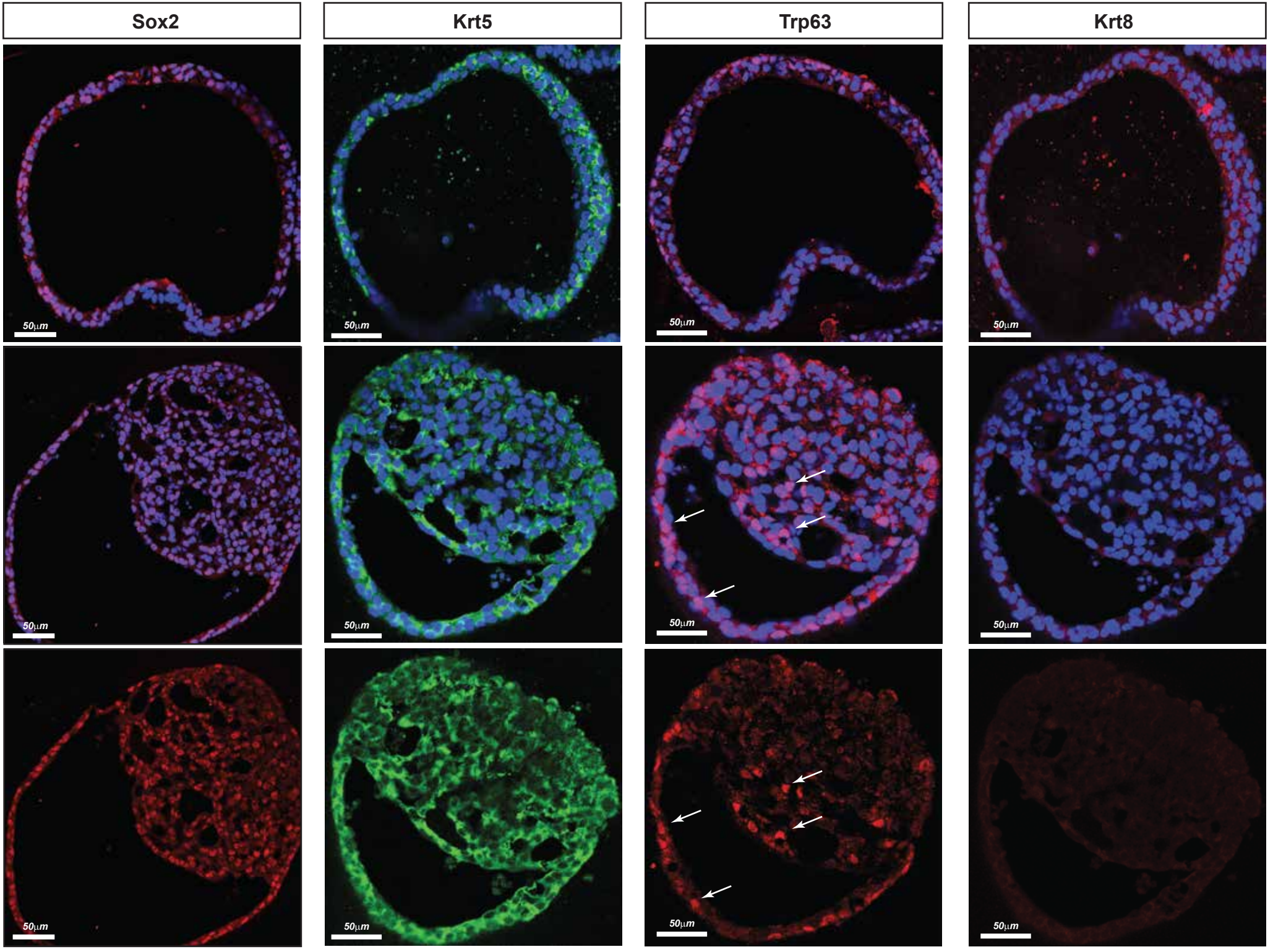
Sox2
Krt5
Trp63
Krt8
Vehicle
BCL11A^ovx
BCL11A^ovx
50μm

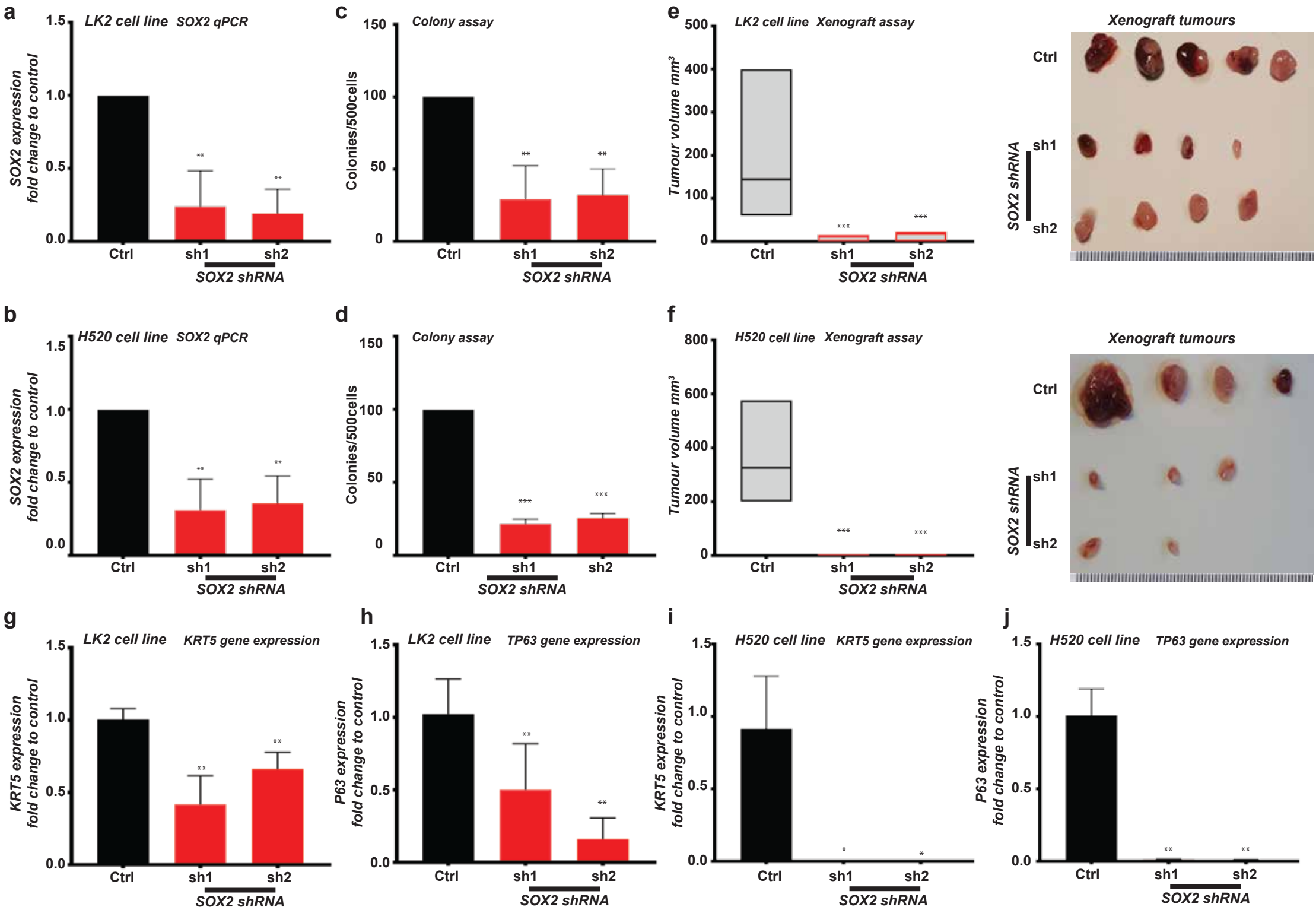
a
LK2 cell line SOX2 qPCR
SOX2 expression fold change to control
1.5
1.0
0.5
0.0
**
**
Ctrl
sh1
sh2
SOX2 shRNA
c
Colony assay
Colonies/500cells
150
100
50
0
**
**
Ctrl
sh1
sh2
SOX2 shRNA
e
LK2 cell line Xenograft assay
Tumour volume mm3
500
400
300
200
100
0
***
***
Ctrl
sh1
sh2
SOX2 shRNA
Xenograft tumours
Ctrl
SOX2 shRNA
sh1
sh2
b
H520 cell line SOX2 qPCR
SOX2 expression fold change to control
1.5
1.0
0.5
0.0
**
**
Ctrl
sh1
sh2
SOX2 shRNA
d
Colony assay
Colonies/500cells
150
100
50
0
***
***
Ctrl
sh1
sh2
SOX2 shRNA
f
H520 cell line Xenograft assay
Tumour volume mm3
800
600
400
200
0
***
***
Ctrl
sh1
sh2
SOX2 shRNA
Xenograft tumours
Ctrl
SOX2 shRNA
sh1
sh2
g
LK2 cell line KRT5 gene expression
KRT5 expression fold change to control
1.5
1.0
0.5
0.0
**
**
Ctrl
sh1
sh2
SOX2 shRNA
h
LK2 cell line TP63 gene expression
P63 expression fold change to control
1.5
1.0
0.5
0.0
**
**
Ctrl
sh1
sh2
SOX2 shRNA
i
H520 cell line KRT5 gene expression
KRT5 expression fold change to control
1.5
1.0
0.5
0.0
*
*
Ctrl
sh1
sh2
SOX2 shRNA
j
H520 cell line TP63 gene expression
P63 expression fold change to control
1.5
1.0
0.5
0.0
**
**
Ctrl
sh1
sh2
SOX2 shRNA

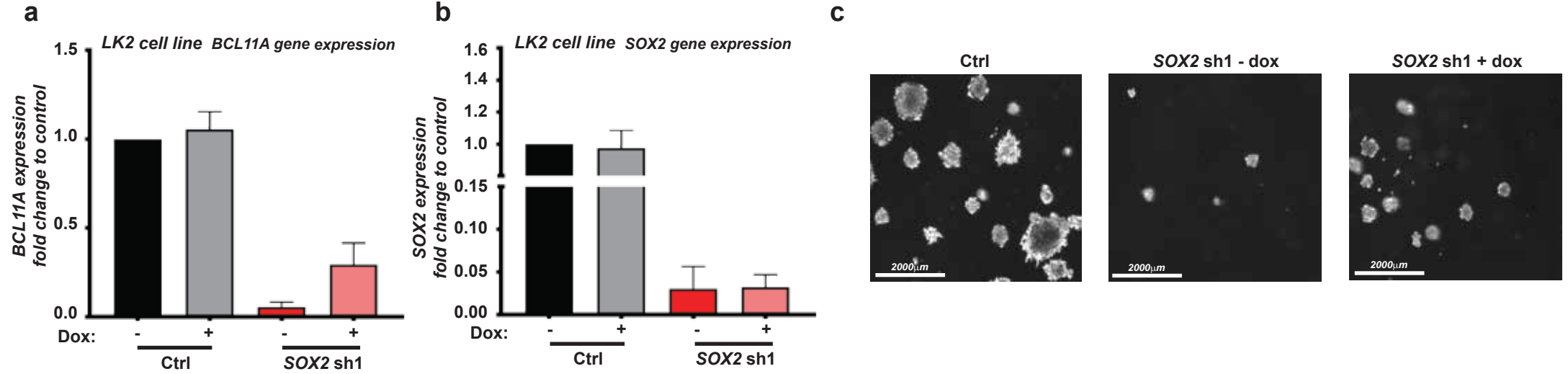
a
LK2 cell line BCL11A gene expression
BCL11A expression
fold change to control
1.5
1.0
0.5
0.0
Dox:
-
+
-
+
Ctrl
SOX2 sh1
b
LK2 cell line SOX2 gene expression
SOX2 expression
fold change to control
1.6
1.4
1.2
1.0
0.15
0.10
0.05
0.00
Dox:
-
+
-
+
Ctrl
SOX2 sh1
c
Ctrl
SOX2 sh1 - dox
SOX2 sh1 + dox
2000μm
2000μm
2000μm

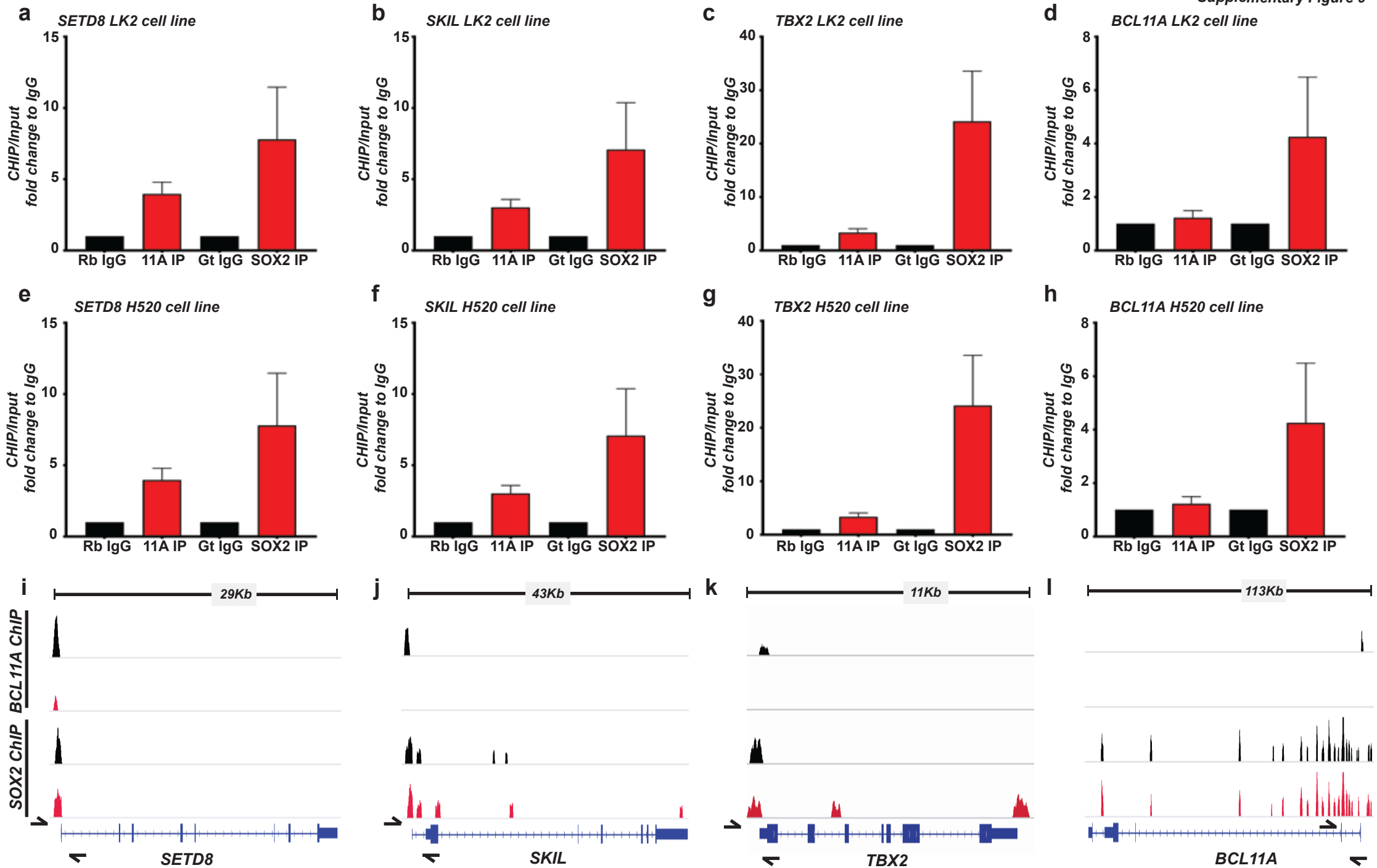
a
SETD8 LK2 cell line
b
SKIL LK2 cell line
c
TBX2 LK2 cell line
d
BCL11A LK2 cell line
e
SETD8 H520 cell line
f
SKIL H520 cell line
g
TBX2 H520 cell line
h
BCL11A H520 cell line
CHIP/Input fold change to IgG
Rb IgG
11A IP
Gt IgG
SOX2 IP
i
29Kb
j
43Kb
k
11Kb
l
113Kb
BCL11A ChIP
SOX2 ChIP
SETD8
SKIL
TBX2
BCL11A

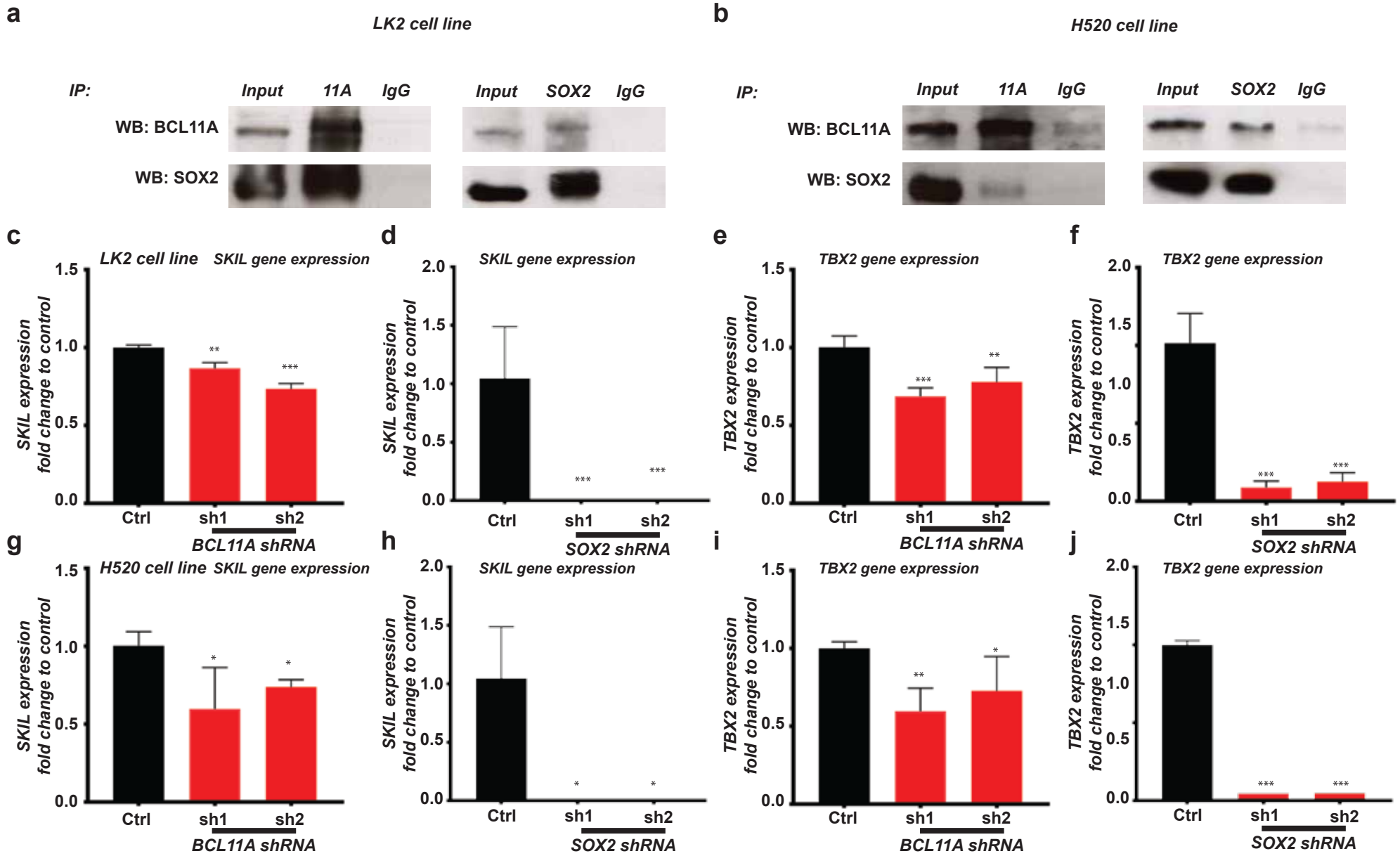
a
LK2 cell line
IP:
Input
11A
IgG
Input
SOX2
IgG
WB: BCL11A
WB: SOX2
b
H520 cell line
IP:
Input
11A
IgG
Input
SOX2
IgG
WB: BCL11A
WB: SOX2
c
LK2 cell line SKIL gene expression
SKIL expression fold change to control
Ctrl
sh1
sh2
BCL11A shRNA
d
SKIL gene expression
SKIL expression fold change to control
Ctrl
sh1
sh2
SOX2 shRNA
e
TBX2 gene expression
TBX2 expression fold change to control
Ctrl
sh1
sh2
BCL11A shRNA
f
TBX2 gene expression
TBX2 expression fold change to control
Ctrl
sh1
sh2
SOX2 shRNA
g
H520 cell line SKIL gene expression
SKIL expression fold change to control
Ctrl
sh1
sh2
BCL11A shRNA
h
SKIL gene expression
SKIL expression fold change to control
Ctrl
sh1
sh2
SOX2 shRNA
i
TBX2 gene expression
TBX2 expression fold change to control
Ctrl
sh1
sh2
BCL11A shRNA
j
TBX2 gene expression
TBX2 expression fold change to control
Ctrl
sh1
sh2
SOX2 shRNA

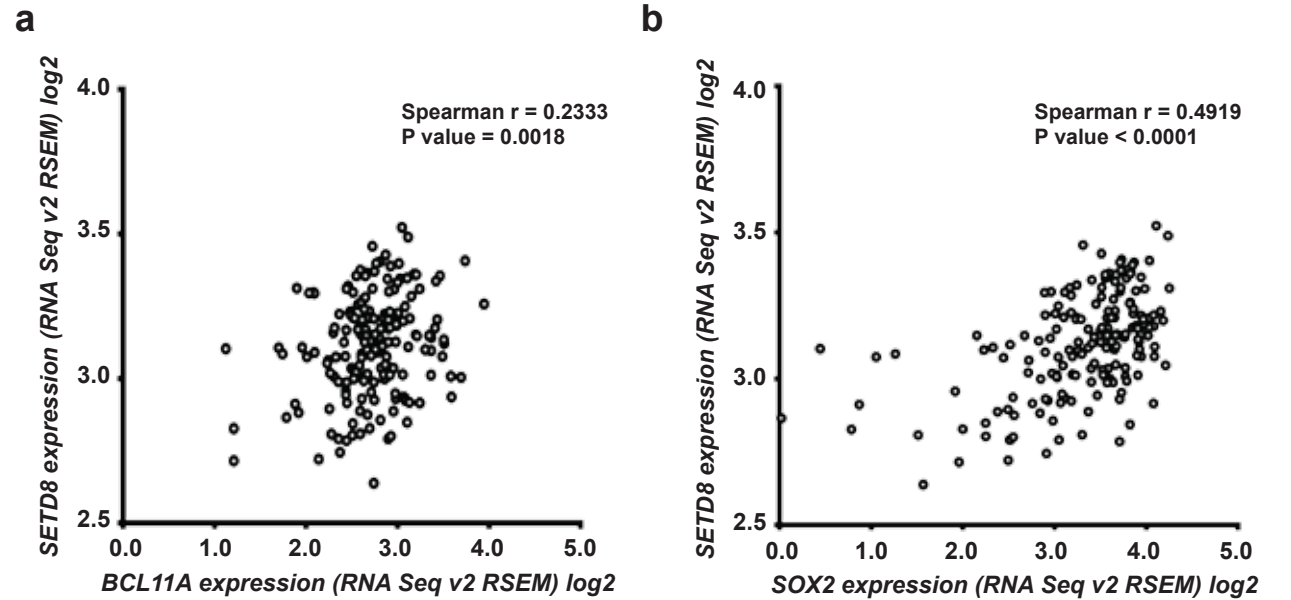
a
Spearman r = 0.2333
P value = 0.0018
SETD8 expression (RNA Seq v2 RSEM) log2
BCL11A expression (RNA Seq v2 RSEM) log2
4.0
3.5
3.0
2.5
0.0
1.0
2.0
3.0
4.0
5.0
b
Spearman r = 0.4919
P value < 0.0001
SETD8 expression (RNA Seq v2 RSEM) log2
SOX2 expression (RNA Seq v2 RSEM) log2